HIPPOCAMPAL REPLAY IN A NOVEL ENVIRONMENT: INFORMATION CONTENT AND INTERACTION WITH PREFRONTAL NEURONAL ACTIVITIES

by

Xiaojing Wu

A dissertation submitted to Johns Hopkins University in conformity with the requirements for the degree of Doctor of Philosophy

Baltimore, Maryland

March, 2014

© Xiaojing Wu
All Rights Reserved

Abstract

Hippocampal place-cell replay has been proposed as a fundamental mechanism of learning and memory, which might support navigational learning and planning. An important hypothesis of relevance to these proposed functions is that the information encoded in replay should reflect the topological structure of experienced environments, that is, which places in the environment are connected with which others. Here we report several attributes of replay observed in rats exploring a novel forked environment that support the hypothesis. First, we observed that spatially overlapping replays depicting divergent trajectories through the fork recruited the same population of cells with the same firing rates to represent the common portion of the trajectories. Second, replay tended to be directional and to flip the represented direction at the fork. Third, replay-associated sharp-wave-ripple events in the local field potential exhibited substructure that mapped onto the maze topology. Thus the spatial complexity of our recording environment was accurately captured by replay: the underlying neuronal activities reflected the bifurcating shape, and both directionality and associated ripple structure reflected the segmentation of the maze. Moreover, we observed that replays occurred rapidly after small numbers of experiences. To further investigate the potential role of sequence replay in cross-structural network functions, we addressed the question of whether and how hippocampal replay interacts with prefrontal processes. We found strong modulations of simultaneously recorded medial prefrontal neuronal activities by running direction on track arms as well as reward conditions at arm ends, indicating their active involvement in task performance. Importantly, prefrontal neurons exhibited

substantial firing-rate changes consistently at the occurrences of hippocampal replay, with a subset of neurons showing significantly different response patterns to replays representing different arms of the maze. Our results suggest that hippocampal replay rapidly captures learned information about environmental topology to support a role in navigation, possibly through informing prefrontal activities in spatial decision making processes.

Thesis advisor:	Dr. David Foster
Official referee:	Dr. Jim Knierim
Other readers:	Dr. Ed Connor
	Dr. Peter Holland
	Dr. Marshall Shuler

Acknowledgements

I would like to sincerely thank my advisor Dr. David Foster for his continued support and guidance; my thesis committee members Drs. Jim Knierim (chair), Ed Connor, Peter Holland, and Marshall Shuler, as well as the students and postdocs in our lab for helpful discussions and comments on our work; Dr. Brad Pfeiffer and Ellen Ambrose for their help with collecting the pre-behavioral sleep data presented in Chapter 3; and my family and friends for their love, friendship, and support. We also wish to acknowledge the support of the Alfred P Sloan Foundation, Whitehall Foundation, and NIH grant RO1 MH085823.

TABLE OF CONTENTS

CHAPTER 1 BACKGROUND 1

1.1 The hippocampus is important for episodic memory formation and long-term storage 2

1.2 Place-cell replay may serve as fundamental mechanism of hippocampal functions 7

1.3 A functional hippocampal-prefrontal network 14

CHAPTER 2 GENERAL METHODOLOGY 19

2.1 Electrophysiology and behavioral task 19

2.2 Position linearization and place field computation 23

2.3 Candidate events and trajectory-specific subregions 23

2.4 Replay identification 25

Figure 2.1 27
Figure 2.2 28
Figure 2.3 29

CHAPTER 3 HIPPOCAMPAL REPLAY CAPTURES THE UNIQUE TOPOLOGICAL STRUCTURE OF A NOVEL ENVIRONMENT 31

3.1 Specific aim 31

3.2 Quantification methods 32

3.2.1 Cumulative replay numbers and place field modular shuffle 32

3.2.2 Comparison of cell activities in joint replay common segments 33

3.2.3 Directionality of replay 34

3.2.4 Ripple and multi-unit activity analyses 35

3.3 Results 36

3.3.1 Abundant joint replays spanning each two connecting arms were identified 37

3.3.2 Multiple trajectories were replayed in the same stopping period 38
3.3.3 Neuronal sequences were bifurcated 39
3.3.4 Replays were highly directional 40
3.3.5 Ripples were specifically associated with arms during joint replays 42
3.3.6 Joint replays were detected after little experience 44
3.4 Discussion 45
3.4.1 Y maze structure was captured by individual neuron and population activities 45
3.4.2 Implications of joint replay directionality 47
3.4.3 Rapid occurrence of joint replays 49
3.4.4 The phenomenon of 'preplay' 50
Figure 3.1 53
Figure 3.2 55
Figure 3.3 56
Figure 3.4 58
Figure 3.5 60
Figure 3.6 61
Figure 3.7 63
Figure 3.8 65
Figure 3.9 67
CHAPTER 4 ACTIVITY CHANGES OF MEDIAL PREFRONTAL NEURONS COINCIDENT WITH HIPPOCAMPAL REPLAY EVENTS DEPENDED ON REPLAY REPRESENTATION 69
4.1 Quantification methods 69
4.1.1 Selection of mPFC single units 70
4.1.2 Running direction modulation of mPFC neuronal activities 70
4.1.3 Medial prefrontal neuronal activities at replay occurrence 71
4.1.4 Statistical analysis 72
4.2 Results 73

4.2.1 CA1 replays representing different paths were detected in abundant numbers 74
4.2.2 Running direction modulated mPFC neuronal activities 74
4.2.3 Reward conditions affected mPFC activities 76
4.2.4 Change of medial prefrontal activities upon replay occurrence 77
4.2.5 Replay – mPFC coactivity depended on replay content 78
4.3 Discussion 81
4.3.1 Medial prefrontal activities were modulated by important task components 81
4.3.2 The possible role of mPFC – hippocampal replay interaction in decision making 82
4.3.3 Network mechanisms involved in the interaction between prefrontal activities and hippocampal replay 84
Figure 4.1 86
Figure 4.2 87
Figure 4.3 89
Figure 4.4 91
Figure 4.5 93
Figure 4.6 95
CHAPTER 5 GENERAL DISCUSSION 97
Figure 5.1 105
Figure 5.2 106
REFERENCES 107

Chapter 1 Background

Learning and memory are among the most fundamental neural processes that play significant roles in a wide array of behaviors. As many other nervous system functions, learning and memory take many forms in many different organisms. The simplest form may be habituation in invertebrate animals, such as reduction in defensive withdrawal reflexes of *Aplysia*'s gill and siphon to repeated stimuli. Its mechanism has been traced to activation of signaling cascades in both the presynaptic sensory neurons and postsynaptic motor neurons, regulated by modulatory inputs from serotonergic interneurons, resulting in changes in sensorimotor synaptic strength (Owen & Brenner, 2012). Such 'cellular learning', although simple, is important for understanding how cellular activities induce actual changes in behavior. For humans and other vertebrate animals, learning and memory are described as 'cognitive processes' because they involve processing of (sometimes abstract) information. The high level of complexity of human memory is reflected in frameworks proposed by, *e.g.* (Rugg *et al.*, 2008) which suggested mechanisms of how memories composed of different types of information may be stored in distinct brain areas, and how partial cues may elicit reactivation of involved brain structures and successful retrieval of complete memories. Meanwhile, new properties of human learning are still being discovered. For example, (Yoo *et al.*, 2012) found that learning during brain states corresponding to low level of activity in the parahippocampal cortex improved recall of previously viewed novel scenes. Mainly employing noninvasive methods such as functional magnetic resonance imaging, transcranial magnetic stimulation, and experimental psychology, human studies aim to understand

learning and memory at the behavioral and brain-structure level, representing the other end of the spectrum. In this thesis, we focus on an 'in between' level of research in an 'in between' animal model, with the goal of understanding at the neuronal ensemble level, how novel information is encoded and utilized to guide behavior. Uncovering representations and functional consequences of coordinated firing activities across individual neurons within and between brain areas is essential for understanding mechanisms of information processing in the brain, and for bridging knowledge gained at the synaptic level to the broad-scale brain-structure level to achieve a complete understanding of learning and memory.

1.1 The hippocampus is important for episodic memory formation and long-term storage

Previous studies have generated a large body of knowledge about the brain structures responsible for learning and memory, and physiological properties of the neurons and their synaptic connections within these structures. Initially discovered from examining amnesic and schizophrenic patients (Scoville & Milner, 1957; Corkin *et al.*, 1997), it has been strongly suggested that the hippocampal formation and surrounding cortical structures in the medial temporal lobe support a distinct memory function – the establishment of initial and long-term storage of information as associated with specific contexts such as events taking place at particular times and places (Squire, 1992; Eichenbaum, 2013). This episodic memory is distinct in information content from other classes of memory, namely semantic memory concerning facts independent of context, and procedural memory mainly involving motor skill learning. Having distinguished

between different types of memory, the significance of episodic memory becomes clear: organisms are constantly interacting with the outside world and adjusting their behaviors according to previous successes and failures to enhance the chance of survival; the ability to learn through personal experiences and the brain capacity of episodic memory formation are thus useful means for acquiring knowledge and guiding behavior. From this point of view, when studying the mechanism of episodic memory questions should be asked about how 'raw' inputs streaming into the brain from experiences are encoded, manipulated, and eventually integrated and utilized to guide or alter behavior.

Several properties of the hippocampus have been revealed which support its role in learning and memory. Anatomically, the hippocampus is at the highest level of a hierarchy of brain structures and receives 'end-stage' information from various sensory and associative cortices, as well as inputs from the subcortical neuromodulatory nuclei, further processed by the perirhinal, parahippocampal and entorhinal cortices (Mishkin *et al.*, 1998; Andersen *et al.*, 2006). Receiving such highly processed and converged information, it is at an ideal position to orchestrate the formation of episodic memory which is characterized by its high-dimensional sensory modalities. Synaptic plasticity is another major property of the hippocampus where the significant discovery of long-term potentiation (LTP) was first made, in both anesthetized and awake rabbits (Bliss & Gardner-Medwin, 1973; Bliss & Lomo, 1973). It is a phenomenon whereby excitatory postsynaptic potentials elicited by single-pulse stimuli to the presynaptic axons are enhanced after delivery of a train of high-frequency stimuli to the same axons, which lasts from several minutes to months (Abraham, 2003). LTP, together with the later

discovered opposite phenomenon long-term depression (LTD) (Lynch *et al.*, 1977), demonstrate that the strengths of synaptic connections among neurons can be up- or down-regulated according to their firing activities. Intensively studied for their potential roles in cellular mechanisms of information storage, both phenomena have been found at virtually every synapse in the hippocampus: synapses between the perforant path and granule cells in the dentate gyrus, the Schaffer collateral to CA1 pyramidal cell synapses, recurrent connections among CA3 cells, *etc.*, reinforcing the idea that the hippocampus is an important brain area for learning and memory.

Investigating the representations of single neuron activities has been the principal method for studying many brain structures. Single units in the human hippocampus were shown to be selectively activated by different photographs of the same actress, landmark building, *etc.*, and even letter strings of their names, reflecting encoding of explicit memories and learned abstract concepts (Quiroga *et al.*, 2005). While this striking finding provides direct evidence for hippocampal neurons' role in memory, this representation might be unique to only humans and non-human primates. Experiments conducted in freely moving rodents discovered a more universal phenomenon: during continuous exploration of a spatial environment, each active neuron in the hippocampus exhibits pronounced firing activities only when the animal traverses a specific location in the environment, while firing rates outside the location are virtually zero (O'Keefe & Dostrovsky, 1971). For rats and mice, such place responses were shown in pyramidal cells in the CA1 and CA3 subfields, and in granule cells in the dentate gyrus, which were consequently termed place cells with their firing fields termed place fields (Moser *et al.*,

2008). Place and place-related responses have been further reported in monkeys (Matsumura *et al.*, 1999), humans (Ekstrom *et al.*, 2003), and flying bats (Yartsev & Ulanovsky, 2013).

Since spatial selectivity is such a prominent neurophysiological property of the hippocampal neurons, the function of the hippocampus cannot be understood without clear interpretation of place responses. On one hand, place fields may be viewed as spatial representations of locations resulting from direct sensory inputs into the hippocampus that characterize 'space', thus analogous to the receptive fields of visual neurons. On the other hand, place responses may be interpreted as a neuronal basis of spatial learning and memory (Olton & Samuelson, 1976; O'Keefe & Nadel, 1978): the cognitive map theory outlines the construction of an allocentric mental map of the environment by acquisition and accumulation of spatial information gained through egocentric experience within the environment. All sensory inputs (vision, audition, olfaction, proprioception, directional cues, *etc.*) are integrated to derive navigationally useful information such as relative locations among landmarks and their attributes, which can be recalled to create novel routes and to guide navigation. The role of place cells in map generation is still unclear. They have been suggested to receive positional and directional information computed through path integration mechanisms in the entorhinal cortex, to provide better interpreted information about the environment by signaling current location with respect to the environment, or by encoding distal or local landmarks or both (Jacobs & Schenk, 2003; McNaughton *et al.*, 2006). From this point of view, place cells may be hypothesized to encode the memory of a location instead of the

perception of it, which might require specific intrinsic hippocampal mechanisms to transform the direct sensory inputs into conceptualized representations of locations. In support of this view, it was found in open field environments that place cell activities were invariant to rats' orientation within the place fields despite the different sensory stimuli they were facing at different orientations (O'Keefe & Dostrovsky, 1971; O'Keefe, 1976; Bird & Burgess, 2008); furthermore, some place cells were found to maintain their place fields in complete darkness (Quirk *et al.*, 1990).

In general, however, it is hard to definitively conclude whether place responses require any learning because the encoding stimulus – place – must be present at the time of retrieval. It has been shown that many place cells began to fire within their steady-state place fields upon the animal's very first entry into the place field locations (Hill, 1978), while (Wilson & McNaughton, 1993) indicated that the stabilization of place fields took about 10 min of experience in the novel environment. A more recent and more sophisticated analysis showed that although most CA1 cells were active during the first passage of a novel arm, place fields exhibited rapid changes during the initial moments of exposure and required at least 5-6 min of experience to stabilize (Frank et al., 2004). Albeit a good indicator for learning requirements, it is difficult to estimate the time course of development of place fields since place field calculation requires the accumulation of spike and position data. Interestingly, (Frank *et al.*, 2004) also showed that even though place fields had become stabilized on the third day of exposure to the novel arms, the rats continued to run at a slower speed on those arms on day three than they did on the familiar arms, indicating that they did not treat the novel arms as familiar

even when place fields were already stable. They suggested that 'although the hippocampus may form new memories quickly, using those memories to guide behavior also requires changes in other brain regions'. Thus, it is still unknown how much navigation relies on hippocampal spatial representation at the earliest stage of spatial learning. It should be noted that in spite of the controversies in interpretations of place responses, all views recognize the possibility that the hippocampus may function as an information integrator. Major theories, such as the Relational Theory (Cohen, 1993), Marr's pattern completion theory (Marr, 1971), and the Byrne, Becker and Burgess model (the BBB model, (Byrne *et al.*, 2007)) all point to a role of the hippocampus in the convergence and flexible association of incoming information from different neocortices, emphasizing the spatial aspect of the integration: the geometry of the environment, the features and locations of the objects within, the environmental boundaries, *etc.* (Bird & Burgess, 2008).

1.2 Place-cell replay may serve as fundamental mechanism of hippocampal functions

The discoveries of LTP and LTD, and subsequently spike-timing-dependent plasticity, provided strong support to the Hebbian theory that when a certain firing pattern across an assembly of neurons occurs repeatedly, synaptic connections among the participating neurons will be selectively strengthened or weakened depending on the temporal order in which pre- and postsynaptic spikes were fired (Hebb, 1949; Allport, 1985; Dan & Poo, 1992). Although the precise synaptic mechanisms may be different for different brain systems, model organisms, or different forms of learning, the general idea that learned

information may be stored as modified synaptic connections has prevailed. (Wilson & McNaughton, 1994) first discovered that place cell pairs showing high spike-train cross-correlations during spatial foraging tasks due to their overlapping place fields also exhibited high levels of coactivity during the sleep periods after waking behaviors, which were significantly enhanced from the sleep periods prior to behavior; place cell pairs with non-overlapping place fields were not coactive during either waking behavior or either of the sleep sessions. This reoccurrence of cell pair-wise correlations during post-behavioral sleep was found to mainly occur during sharp-wave ripple (SWR) events detected in the local field potential (LFP) signals and believed to reflect synchronous synaptic inputs from the CA3 to CA1 as well as population firing activities in both subareas (Csicsvari *et al.*, 2000), and was interpreted as reactivation of stored activity patterns in an 'auto-associative' neuronal network formed during behavior through synaptic modifications within the hippocampus. The authors further suggested that the 'play back' of waking neuronal patterns during subsequent sleep may contribute to memory consolidation, a process in which information initially stored in the hippocampus is gradually transferred to the neocortices for long-term storage, an idea first introduced by the noted Roman teacher of rhetoric, Quintillian (Muller & Pilzecker, 1900; Dudai, 2004). This finding of ripple-associated reactivation primarily during slow-wave sleep and its proposed role in memory consolidation have been repeated and supported by numerous studies (Skaggs & McNaughton, 1996; Kudrimoti *et al.*, 1999; O'Neill *et al.*, 2006; O'Neill *et al.*, 2008; Nakashiba *et al.*, 2009).

Many subsequent studies extended this discovery by demonstrating that the sequential order in which place cells become active during running experiences due to the orderly traversal across their place fields, was reactivated during not only post-behavioral sleep but also awake immobile periods when rats eat, drink, groom, rest, or briefly pause between episodes of exploratory behaviors, producing extended spiking sequences across place cell ensembles that match sequences from previous behavioral episodes, often in a temporally condensed form during 100-200 ms sharp-wave ripple events (Louie & Wilson, 2001; Lee & Wilson, 2002; Foster & Wilson, 2006; Csicsvari *et al.*, 2007; Diba & Buzsaki, 2007; Ji & Wilson, 2007; Davidson *et al.*, 2009; Karlsson & Frank, 2009; Gupta *et al.*, 2010). The observation of sequence replay is consistent with that of the reactivation of pair-wise correlations, which demonstrate the same fine time-scale firing orders exhibited by cell pairs drawn from complete sequences that are ultimately determined by the spatial relationship of their place fields – both can in fact provide statistics for the measurement of how much reactivation activities match waking experiences (Karlsson & Frank, 2009). On the other hand, extended sequences contain more information than pair-wise correlations, such as whole trajectories and heading directions (see below) represented in the reactivation event, the speed of trajectory replay, *etc*. An effective Bayesian decoding algorithm has been developed to greatly improve visualization and detection of replay events, and has been used to accurately characterize replay sequences representing almost the entire length of a ten-meter long track (Davidson *et al.*, 2009).

The establishment of sequence replay has also been suggested to rely on synaptic plasticity, which has been explored by several computation modeling studies (Jensen & Lisman, 1996; Levy, 1996; Leibold & Kempter, 2006; Molter *et al.*, 2007; Koene & Hasselmo, 2008). For example, a model developed by (Molter *et al.*, 2007) was structured in a two-stage manner first proposed by (Buzsaki, 1989), whereby sequence memory first becomes (weakly) encoded in the hippocampal circuits through synaptic modifications induced during running when the hippocampus engages in prominent theta oscillations (4-12 Hz), and is later manifested in a different brain state during hippocampal SWRs which may allow further potentiation of established synaptic connections. More specifically, the phase precession property, that in the course of place field traversal the phase of place cell firing in relation to the ongoing theta rhythm progressively shifts to earlier phases in each successive theta cycle, could confine spikes from place cells with overlapping place fields to always occur in the same order within a small time window; based on the time asymmetric Hebbian learning rule (Levy & Steward, 1983; Dan & Poo, 1992), recurrent synaptic connections from a given CA3 place cell to the CA3 cells with the next place field can be consequently strengthened. In the subsequent immobile state, CA3 units receive irregular and either nonspecific or biased inputs such that either all units have the same probability of getting activated or units with place fields covering the current location have increased probability of becoming activated. The first-active unit then initiates a train of firing activities across those units connected via potentiated recurrent synapses which become sequentially activated, in the form of sequence replay. Essential for this class of theoretical analyses is the hypothesis that rapid plastic changes in the CA3 recurrent network is a fundamental

mechanism of hippocampal replay, which has been supported by (Nakazawa *et al.*, 2003) showing that NMDA receptors in the CA3 pyramidal neurons were required for both one-time fast learning of spatial behavioral tasks and normal place cell encoding of novel environments.

While SWR-associated place-cell sequences, just as the reactivation of place-cell pair-wise correlations, have been interpreted as a mechanism for "replaying" neuronal representations of previous experiences for the purpose of memory consolidation, particularly during sleep (Girardeau *et al.*, 2009; Ego-Stengel & Wilson, 2010; O'Neill *et al.*, 2010; Carr *et al.*, 2011), there is growing evidence that they also contribute to navigational learning and planning (Diba & Buzsaki, 2007; Buckner, 2010; Foster & Knierim, 2012), the difference being faithful engram of a novel spatial experience 'as it is', versus further information processing by the brain and flexible use of the derived 'secondary information' for guiding behavior. Place-cell sequences occur during the awake state during pauses in behavior at reward sites, in which the previously experienced behavioral sequence is replayed in not only the same (forward) order, but also surprisingly the opposite (reverse) order (Foster & Wilson, 2006; Diba & Buzsaki, 2007; Davidson *et al.*, 2009; Karlsson & Frank, 2009), and in a manner likely to be modulated by reward outcomes such that receipt of reward may enhance replays of paths leading to reward (Singer & Frank, 2009), hence providing an ideal representation for associating locations with graded predictions of expected future reward (Montague *et al.*, 1996; Foster & Wilson, 2006). More recently, it has been demonstrated that SWR-associated place-cell sequences occurring immediately prior to movement in a spatial

memory task depict the future trajectory that the animal will take to the remembered goal location (Pfeiffer & Foster, 2013). Therefore, hippocampal SWR-associated place-cell sequences might provide a mechanism by which the brain addresses the learning, memory, and planning demands inherent in memory-based navigation (Tolman, 1948; O'Keefe & Nadel, 1978).

It should be noted that studies prior to the discovery of reactivation activities had already demonstrated learning-related changes in hippocampal neural responses. At the synaptic level, it has been shown that one-trial inhibitory avoidance learning enhanced field excitatory postsynaptic potential slope in CA1 (Whitlock et al., 2006), and that exploration of a novel environment rapidly induced a persistent reversal of high-frequency stimulation-induced long-term potentiation in CA1 (Xu et al., 1998). On the level of single place cell activities, (Mehta et al., 2000) reported a backward skewing of place field shape and an increase in place field size during repeated traversal on linear tracks within the same recording session; (O'Keefe, 1976; Hollup *et al.*, 2001) observed that previously silent cells formed new place fields after a sudden change in the environment; (Muller & Kubie, 1987) demonstrated changes in place fields in various ways following different manipulations of the recording environment; long-term changes were shown as place cells started to distinguish between a familiar and a novel cue card across recording sessions (Bostock et al., 1991), or a circular environment and a square environment across days (Lever et al., 2002). These interesting findings provided strong evidence to the general understanding that the hippocampus responds quickly and often with persistent changes to experience, or anything novel the animal may encounter in its

environment, although their relationships with replay are still unclear. Changes in synaptic activities, as discussed earlier, may underlie formation or modification of replay which in turn may provide sufficient temporal contingencies for further potentiation of specific synapses; changes in place fields most likely alter replay representation which can be decoded by using each place cell's place responses in the entire environment (Davidson *et al.*, 2009), while replay may also play a role in the formation and stabilization of place fields which might be updated within the same spatial experience through mechanisms occurring during awake replays. A further plausible hypothesis may be that learning mechanisms within the hippocampus might not be necessary in certain situations for acquiring place fields (Hill, 1978), but might always be necessary for configuring rapidly the relationships between place fields as expressed in replay. It should be recognized that sequence replay is the only form of hippocampal activity that reflects learning-induced changes at the level of coordinated neuronal ensemble activities and clearly depicts spatial relationships among single neuron representations as well as extended episodes of experiences, while research at all levels need to be continued to achieve a complete understanding of hippocampal processes.

Finally, many important studies contributing to the discovery and characterization of place-cell sequence replay have used linear tracks (Foster & Wilson, 2006; Diba & Buzsaki, 2007; Davidson *et al.*, 2009), which however oversimplify real-world situations. Complex environments, in particular those composed of branching structures, together with more complex spatial behavioral tasks, have been used to study replay. These experimental paradigms have yielded novel properties and significant insights about

replay. For example, (Karlsson & Frank, 2009) discovered prevalently occurred remote replays of the previous environment when rats were exploring the current environment, using W-shaped mazes; (Gupta et al., 2010) used a two-choice T maze and found that the frequency of a trajectory being replayed did not simply follow the recency or frequency of the experiences of that trajectory. As research is progressing to attempt to address more complicated questions about replay, complex environments may become increasingly desirable for providing sufficient spatial complexities and behavioral contingencies, depending on the specific questions of interest.

1.3 A functional hippocampal-prefrontal network

The roles of the hippocampus in important behaviors such as spatial navigation can be summarized as learning and encoding detailed spatial information, plus possibly other associated features such as reward information, about the navigational environment, and displaying such information in a manner suitable for action planning. To accomplish the navigation behavior, involvement from other brain areas is required for reaching the final decision for the next destination or desired route. It is crucial to understand what and how hippocampal output is utilized by these brain regions, which however remains largely unknown. One brain area responsible for carrying out complex 'executive functions' that involve planning, problem solving, outcome prediction, *etc.*, is the prefrontal cortex, which has been intensively studied in humans and non-human primates. Rodents have also been used as animal models for the study of the prefrontal cortex. Although lacking a repertoire of complex behaviors comparable to primates, rodents are certainly able to perform tasks that demand rule learning, reversal learning, response inhibition, working

memory, and decision making (Kesner & Churchwell, 2011). Importantly, strong evidence emerging from rodent studies suggests the existence of a functional hippocampal-prefrontal network. Anatomical examinations revealed reciprocal connections between the two brain areas, including monosynaptic projections from the ventral CA1 to the medial prefrontal cortex (mPFC) (Swanson, 1981; Jay & Witter, 1991; Carr & Sesack, 1996; Thierry *et al.*, 2000). The dorsal CA1 area does not have direct connections with the mPFC, which have been suggested to interact via indirect pathways that involve the ventral CA1, the perirhinal and postrhinal cortices, and the reuniens nucleus of the midline thalamus (Fanselow & Dong, 2010). Lesion studies such as reported in (Wang & Cai, 2006) observed spatial memory deficits after disconnection of the network, *e.g.* by contralateral muscimol injections which deactivate either brain region in both hemispheres. Lesions to the mPFC or the hippocampus alone also impair spatial navigation, spatial memory, and goal-directed behaviors (Floresco *et al.*, 1997; De Bruin *et al.*, 2000; Brown & Bowman, 2002; Jones, 2002; Vertes, 2006). Neurophysiology experiments further demonstrated, at the neuronal network level, coordinated activities between the two structures in both important states of hippocampal activities (Buzsaki, 1989): during engagement in various spatial navigation tasks, spike trains of medial prefrontal single neurons are phase locked to hippocampal theta rhythm while correlated with firings of CA1 cells in a pairwise manner; coherence between local field potential (LFP) signals also increases and shows significance only in the theta-frequency range. Interestingly, this synchrony can be altered by behavior, and can display significant enhancements during 'choice epochs' demanding working memory and decision making (Hyman *et al.*, 2005; Jones & Wilson, 2005; Siapas *et al.*, 2005;

Benchenane *et al.*, 2010). Similar forms of coactivation were also uncovered during slow-wave sleep (SWS), an important brain state for memory consolidation (Wilson & McNaughton, 1994; Walker & Stickgold, 2006; Rasch & Born, 2013), during which the hippocampus exhibits high-frequency sharp-wave ripple bursts strongly associated with reactivation of previous waking experiences (Wilson & McNaughton, 1994; Kudrimoti *et al.*, 1999; O'Neill *et al.*, 2008; Nakashiba *et al.*, 2009; O'Neill *et al.*, 2010). (Siapas & Wilson, 1998) first reported, during SWS, the co-occurrence of SWRs and mPFC spindles – characteristic slow-wave thalamocortical oscillations (Steriade *et al.*, 1993), and co-firing of CA1 and mPFC neurons around these LFP events.

These fascinating findings established that neural activity synchronization, as manifested by co-occurred cell-pair spikes, entrainment of spikes to LFP rhythms, and coherent or coincident brain wave oscillations, is a fundamental mechanism of hippocampal-prefrontal interaction. Indeed, coactive cell assembly that arise from this synchronization exert greater influences on downstream neurons with simultaneously arrived synaptic inputs, thereby triggering participation of targeted neurons and selectively strengthening synapses according to spike timing-dependent plasticity; such network-wise coordination may be facilitated by broad-scale extracellular voltage fluctuations which may help maintain constant cross-region spike timing differences. This mechanism has been suggested by previous studies to ultimately control the flow and storage of information between brain areas - yet still unclear is the specific information being communicated, which becomes the next important question towards an understanding of the hippocampal-prefrontal network. Recent advancement in multi-tetrode experimental

techniques enabled simultaneous, dual-region recordings of large numbers of neurons, and consequently the decoding of representation emerging at neuronal network level which could not previously be revealed from single neuron activities. By studying ensembles of mPFC neurons, (Peyrache *et al.*, 2009) showed reactivation of coactivation firing patterns of specific mPFC cell assemblies, which emerged during task performance after rule acquisition, during post-training SWS which coincided with hippocampal SWRs. It was suggested that this reactivated pattern represented the newly learned rule, or was 'tagged' by a reward signal, in either case indicative of the information being exchanged in the hippocampal-prefrontal network during SWR epochs.

While the representation of prefrontal neurons always proves difficult to be deciphered, that of hippocampal pyramidal cells appears to be, in most studies, straightforwardly spatial. Hippocampal place cells collectively represent the animal's current location during running; prolonged firing sequences across place cell ensembles resulting from traversals along extended paths up to ten meters in length have been shown in multiple studies to replay in a temporally compressed manner, during not only post-running sleep but also awake immobile periods when rats were pausing on the track (Louie & Wilson, 2001; Lee & Wilson, 2002; Foster & Wilson, 2006; Csicsvari *et al.*, 2007; Diba & Buzsaki, 2007; Ji & Wilson, 2007; Davidson *et al.*, 2009; Karlsson & Frank, 2009; Gupta *et al.*, 2010). Also co-occur with SWRs, place cell replay events have been hypothesized to be an important hippocampal mechanism that plays significant roles in memory consolidation (Foster & Wilson, 2006; Ji & Wilson, 2007; O'Neill *et al.*, 2010; Carr *et al.*, 2011) and planning of future actions (Diba & Buzsaki, 2007; Buckner, 2010). Could

there be any correlations between prefrontal activities and hippocampal replay, which may allow spatial trajectory information important for navigation, now well documented to be explicitly represented by replay, to be exchanged within the network? This correlation would be much more informative than pair-wise correlations between single prefrontal and hippocampal neurons, as the firing of a single hippocampal neuron does not differentiate between different trajectories passing the same location the neuron might be signaling. It should be noted that place cells might also represent non-locational information such as the passage of time or distance travelled (Pastalkova *et al.*, 2008; MacDonald *et al.*, 2011; Kraus *et al.*, 2013), licking and taste (Ho *et al.*, 2011), and emotional factors such as reward, fear, and stress (Moita *et al.*, 2003; Lee *et al.*, 2006; Royer *et al.*, 2010), as revealed in specially designed experiments. As mentioned before, these features are likely encoded in relation to spatial locations in the hippocampal output, the understanding of which, like trajectory replay, should be achieved at the neuronal ensemble level and will also require the use of decoding schemes. Finally, the question of whether correlations exist between trajectory replay and prefrontal activities is also important for understanding place cell replay itself, as its interaction with neuronal processes in other relevant brain areas is indispensable to its proposed roles in complex functions known to demand multiple brain areas working in concert.

Chapter 2 General Methodology

To study place-cell sequence replay and its relationship with concurrent prefrontal neuronal activities, we employed dual-region multi-tetrode recording techniques in awake behaving rats during performance of a spatial navigation task. This chapter describes experimental procedures and quantification methods that formed the basis of this thesis.

2.1 Electrophysiology and behavioral task

Male Long-Evans rats, 3.5-4.5 months in age, were pre-trained to run back and forth on a linear track (~167cm total length) for chocolate milk reward available at both track ends under moderate food deprivation (body weights kept no lower than 85% of original weights). The liquid reward was delivered by the experimenter remotely through long plastic tubings connected to the food wells placed at track ends. The purpose of pre-training was to accustom rats to the routine of running for food reward on a track, which was ended when animals reached the performance criterion of running ~30 laps within 30-40 minutes, usually after 1-2 weeks. Custom designed micro-drives consisting of 40 independently adjustable tetrodes (Figure 2.1) were then implanted with half the tetrodes targeting the right dorsal CA1 area (-3.6mm, -2.2mm from bregma) and the other half targeting the right medial prefrontal cortex (+3.2mm, -0.8mm from bregma). The dura mater was retracted in both craniotomies. Tetrodes entered the brain after travelling through two cannulae at the bottom of the drive which were placed immediately above the exposures and secured with dental cement. During the next 5-12 days post-surgery

tetrodes were gradually advanced into the targeted brain structures by small increments per day while rats slept under bright light in a walled sleep box. Hippocampal tetrodes were moved into the CA1 pyramidal cell layer identified by the appearance of SWRs in the LFP and coincident intensive firing activities, with one tetrode left in the white matter above the cell layer, where the LFP is relatively flat and firing activities are absent, to provide reference signal to other CA1 tetrodes. The rat medial prefrontal cortex can be subdivided into the dorsally located precentral and anterior cingulate cortices, and the prelimbic, infralimbic, and medial orbital cortices in the ventral region, all with specialized functions (Dalley *et al.*, 2004). We specifically targeted the prelimbic subregion as it has been most strongly implicated in cognitive processes and executive functions, with, although a long-standing debate, suggested homology to the primate dorsolateral prefrontal cortex, in addition to well-documented prominent connections with the limbic structures (Preuss, 1995; Vertes, 2006). Adjustment of the mPFC tetrodes was guided by stereotaxic coordinates roughly calculated for each tetrode based on their positioning within the cannula, whereby depth ranges were estimated according to the anterior-posterior and medial-lateral locations of the tetrodes, usually within 2mm-3.5mm from brain surface. Spiking activities were also relied on to gauge tetrode advancement, given that firing activities are very intense in the motor cortex dorsal to most of the medial prefrontal structure, which become much more sparse as tetrodes reach the mPFC. The prefrontal reference tetrode was kept in an adjacent cortical region without spiking activities. During the tetrode adjusting period, rats were initially given free access to food for at least 3 days to allow post-surgery recovery. They were then food deprived again, and re-trained on the pre-training linear track each day while connected to the recording

system. This second phase of pre-training was for the purposes of reacquainting the animals to tracking running as well as accustoming them to performing navigation tasks while being tethered.

When all tetrodes were in position the first recording day began, on which rats were first exposed to a modified Y maze (Figure 2.2). The Y maze was composed of one long arm (145 cm run segment) and two short arms (65 cm run segment) all separated by 120^{o}. Each arm had a wider reward area at the end (16 cm in length), where chocolate milk reward was delivered in the same way as described above. One short arm was chosen to be the central arm; the other two were termed alternating arms. The rat was placed at the baited end of the central arm and was allowed to freely explore the Y maze and rewarded according to an alternation rule: the first arrival at an alternating end was rewarded; thereafter returns to the central arm were rewarded while visits to the alternating arms were only rewarded if the arm identity was different to the last alternating arm rewarded. Two additional rules were imposed: only central arm → alternating arm runs were rewarded while alternating arm → alternating arm runs were unrewarded; only complete laps between reward areas were rewarded, *e.g.* if the rat runs from the central arm to half way of an alternating arm then returns to the central arm it will not be rewarded. This spatial alternation task was chosen because: 1) rats naturally exhibit spontaneous alternation behaviors (Lalonde, 2002), thus allowing brain activities to be examined in a natural behavioral state; 2) recordings can be done without the need of pre-training on the Y maze due to faster learning of a reward rule natural to rats, so that learning-related processes could be captured during the first exposure to the novel environment; 3) normal

performance of this task requires normal functions of both the hippocampus and mPFC as lesions to either area, as well as those abolishing communications between the two areas, were shown to impair performance (Brito *et al.*, 1982; Deacon & Rawlins, 2006; Wang & Cai, 2006; Yoon *et al.*, 2008).

Spiking activities and local field potential signals were recorded (Neuralynx Inc., Bozeman, Montana) and online digitally filtered in different frequency bands (600 – 6000 Hz for spikes and 0.1 – 500 Hz for LFP). Rats' positions were signaled by a red LED and a green LED attached to the drive and were recorded from an overhead camera as X-Y coordinates in each frame. Fine adjustment of the tetrodes was made on each recording day to maximize cell yield, or to search a new group of mPFC neurons, which was completed as least half an hour before recording to ensure stability. Recording sessions lasted 1 - 2.5 hours and were ended when rats stopped running.

Recordings lasted 3-8 days with one session run on each day and were terminated when cell yield became poor. Rats were sacrificed and lesions were made on selected tetrodes (around the boundaries and at the centers of the exposures) by passing current (30 μA for ~5 seconds) through each tetrode. Animals were then perfused with formalin. Brains were removed, sectioned and stained for cresyl violet to verify tetrode recording locations.

The spike data were manually clustered in the software Xclust2 (M Wilson, MIT) mainly based on peak amplitudes. All subsequent data analysis was performed in Matlab (Mathworks, Natick, MA).

2.2 Position linearization and place field computation

Recorded positions were projected onto three lines (defined by the experimenter) aligned with the three arms of the Y maze. The three lines were then concatenated to produce a linear axis (see Figure 3.1 in the next chapter). Non-directional place fields were computed by using all spike data (1.8-1.9 cm position bins; for each bin, firing rate = total # spikes/total occupancy time) and smoothed with a Gaussian filter (SD = 5 bins). Note that firing rates on the three arms were separately smoothed to minimize mis-estimation of place fields around the choice point. Putative interneurons (mean peak-to-trough spike width < 0.34 ms) and neurons with insignificant place fields (peak firing rate on the Y maze <= 1 Hz) were excluded. The rest of the single units were considered putative place cells and were used in the following analyses.

2.3 Candidate events and trajectory-specific subregions

For each recording session, a smoothed spike density function was computed with all spikes from all putative place cells (10 ms time bins; Gaussian filter, SD = 15 ms). Candidate events were defined as epochs of spikes during which spike densities were above the mean of the function, and contained peaks above two standard deviations over the mean. Only candidate events which occurred when rats' speed was slower than 5

cm/s were considered. A Bayesian decoding algorithm (Davidson *et al.*, 2009) was then applied to the candidate events which calculated the probability of the ensemble of neurons representing each position bin during each time bin.

Single-arm replays representing each individual arm and three types of joint replay extended across each pair of arms (C ↔ R, C ↔ L and R ↔ L; Referred to as CR, CL and RL) were considered. To maximize the likelihood of detecting all six types of replay in an unbiased manner, we segmented the posterior probability matrix of each candidate event in both position and time to further define trajectory-specific subregions. Each candidate event was first separated along the position axis into three segments corresponding to the three arms (Figure 2.3). We defined a maximum a priori probability function (MAP) as the largest probability across all positions per time bin, smoothed in time with a Gaussian filter (SD = 10 ms; blue curves in Figure 2.3). Each single-arm segment was then segmented in time and a trajectory-specific subregion was created around the largest peak of MAP to include time bins whose MAP values were above a threshold of five times the chance level, namely $(1/\textit{total \# position bins})\times 5$ (a fixed threshold only dependent on the size of the track and not the quality of neuronal data). The trajectory-specific subregions of the single arms were then combined in pairs to create those of the joint arms which expanded from the earliest to the latest time bins of the two corresponding single-arm subregions and contained all position bins belonging to the two corresponding single arms (Figure 2.3, right). It should be noted that all single- and joint-arm subregions were continuous in time, *i.e.* arm segments were not shifted across time bins so that they could be pieced together to form a longer sequence, thus this

segmentation method does not artificially create coherent coding of one arm and then another.

2.4 Replay identification

To determine if the posterior probabilities within a trajectory-specific subregion gave rise to a replay sequence, the following three variables were calculated:

1. Length of subregion in time.

2. Arm coverage:

A position bin was considered to be represented in the subregion if its largest probability across time is above the threshold $(1/\textit{total \# position bins})\times 5$. The percentage of represented positions out of all positions within the subregion was defined to be the arm coverage.

3. Weighted correlation:

An adapted form of the Pearson's correlation, weighted correlation measures the strength of correlation between the changes in probability values across time and position and utilizes all pixels in the subregion, given by,

Weighted mean: $m(x;w)=\sum_{i=1}^{M}\sum_{j=1}^{N}w_{ij}x_i \Big/ \sum_{i=1}^{M}\sum_{j=1}^{N}w_{ij}$

Weighted covariance: $\mathrm{cov}(x,y;w)=\sum_{i=1}^{M}\sum_{j=1}^{N}w_{ij}(x_i-m(x;w))(y_j-m(y;w)) \Big/ \sum_{i=1}^{M}\sum_{j=1}^{N}w_{ij}$

Weighted correlation: $corr(x,y;w)=\mathrm{cov}(x,y;w)/\sqrt{\mathrm{cov}(x,x;w)\mathrm{cov}(y,y;w)}$

Where x_i is the i^{th} time bin, y_j is the j^{th} position bin, w_{ij} is the probability of pixel (i,j), M and N are the total numbers of time and position bins of a given subregion.

A single-arm subregion was determined to contain the corresponding single-arm replay if the following three criteria were met:

1. Subregion length ≥ 50 ms (5 time bins);

2. Arm coverage > 50%;

3. Absolute weighted correlation > 0.5.

A joint-arm subregion was determined to contain the corresponding joint replay if the following two criteria were met:

1. Absolute weighted correlation > 0.5;

2. Both of the constituent single-arm subregions meet criteria 1 and 2 for single-arm replays and have the same signs of weighted correlation as that of the joint-arm subregion.

Finally, for a candidate event to be considered to contain a single-arm replay, none of the joint-arm subregions should contain any replays; for a candidate event to be considered to contain a joint replay, neither of the other joint-arm subregions should contain any replays.

Figure 2.1

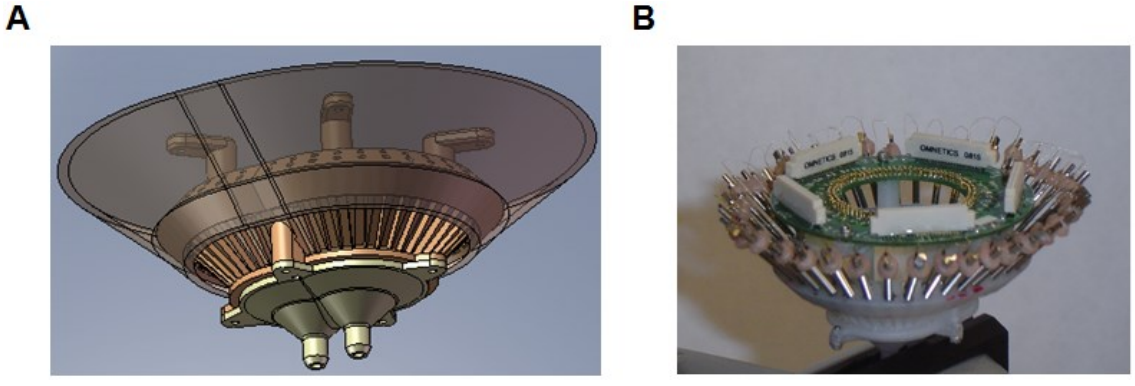

Figure 2.1 Micro-drive for simultaneous dual-region tetrode recordings with 40 independently adjustable tetrodes

(A) Three major structures of the drive, top ring, bottom cannulae, outer shell, were designed in Solidworks (Dassault Systèmes, Waltham, MA), a 3D CAD design software. **(B)** Picture of a completed drive. Tetrode wires were connected to the central electric board with gold pins.

Figure 2.2

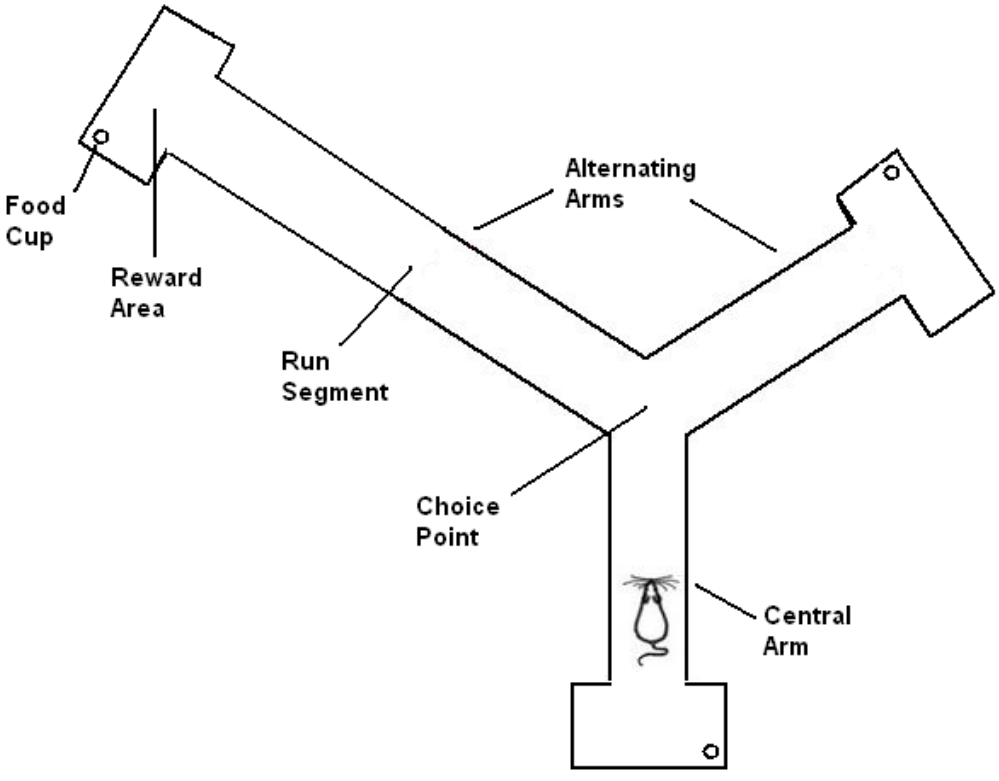

Figure 2.2 Modified Y maze design

The left alternating arm is twice as long as the central arm and the right alternating arm.

Figure 2.3

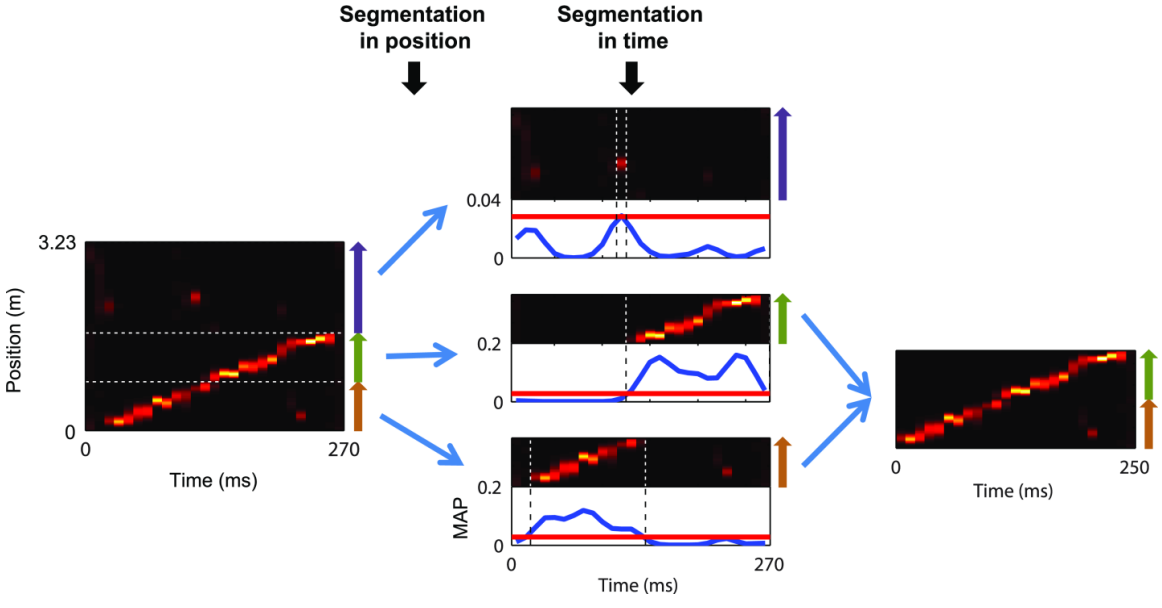

Figure 2.3 Illustration of definition of trajectory-specific subregions within a candidate event for replay detection

An example candidate event (left panel) was first segmented in position, into three segments each corresponding to an individual arm: center top panel, the L arm; center middle panel, the R arm; and center bottom panel, the C arm. Blue curves are MAP functions defined as the largest posterior probability across all positions per time bin, calculated separately for each segment. Vertical dashed lines indicate the windows within which MAPs were above the threshold $(1/\textit{total \# position bins})\times 5$ marked by red lines, thus defining trajectory-specific subregions for the three single-arm segments. In this example, only C and R subregions passed all criteria for containing replay structure,

which were combined to define the subregion for the joint-arm path CR (right panel). This candidate event was finally determined to contain a joint replay of CR.

Chapter 3 Hippocampal replay captures the unique topological structure of a novel environment

3.1 Specific aim

Investigating hippocampal mechanisms important for spatial navigation provides an excellent study system for understanding how brain activities give rise to behavior. A key aspect of the navigation problem is dealing with the topological structure of the terrain, that is, which places are connected to, or accessible from, which other places. This structure determines the set of available paths that can be traversed, as well as the barriers that must be avoided. Navigational schemes that ignore topological structure, such as simple dead-reckoning, can work well in open, unobstructed environments such as those encountered by certain species of desert ant (Gallistel, 1990), but in more complex environments successful navigation is likely to require modes of planning that incorporate topological structure (O'Keefe & Nadel, 1978), to calculate efficient routes to distant goals through non-trivial spatial configurations such as branches or barriers. As discussed in Chapter 1, place-cell sequence replay appears as an ideal candidate for linking discrete locations within the environment in a coherent manner: we hypothesized that hippocampal SWR-associated place-cell sequences would capture the spatial topology of the environment, rather than capturing only the temporal structure of experiences in the environment as independent episodes. The cognitive map theory proposes the same idea that hippocampal representation is achieved through accumulating and integrating information across experiences to encode the environment

'as a whole'. While spatial environments can be defined by many different properties, we focused on hippocampal representation of the topological structure, *i.e.* segmentation of maze-like environments and how different segments are connected and spatially related to one another. We suggest that understanding the true representation of place-cell sequence replay will provide significant insights for understanding the hippocampus.

3.2 Quantification methods

We tested our hypothesis by recording place cell activity while rats explored a novel environment with unpredictable structure: a Y shaped maze with asymmetrical arm lengths. Data from the very first sessions of Rat 1 and 3 are presented in this chapter. Rat 2 did not explore all three arms in his first session (he only made one trip to the reward area of the right alternating arm, ran back to the central arm reward area and stayed there during the rest of the session); data from his second session on the following day is presented here. During periods of time when rats' speed was slower than 5 cm/s, 2514 candidate population spiking events from Rat 1, 3222 from Rat 2, 2902 from Rat 3 were found, within which replay events were identified using methods described in Chapter 2.

3.2.1 Cumulative replay numbers and place field modular shuffle

To quantify replay occurrence, we focused on changes in replay number across stopping periods - periods of time spent between run at a reward area - where the majority of reactivation activities occurred. For each joint replay type, the cumulative number of identified replays was counted for each stopping period, starting from the one immediately following the first lap of traversal across the corresponding arms.

A place field modular shuffle, which circularly shifted each cell's place field by a random number of position bins, was used to determine the stopping period by which the cumulative number of a replay first reached a significant level. This method preserved each cell's spike train and local place field structure. The same algorithm described in Chapter 2 sections 2.3 & 2.4 was applied to cells' shuffled place fields and original spike trains to create sample distributions of cumulative replay numbers (5000 shuffles), from which Monte Carlo *p* values of the original cumulative numbers were calculated. First significant stopping period was defined by $p < 0.05$ (Figures 3.7B-J). The number of laps (running from one arm end to another) of corresponding arm traversals was used to quantify the amount of physical experience acquired before the first significant stopping period. Total numbers of replays in each session, from original and shuffled data, were used for Figure 3.2E.

3.2.2 Comparison of cell activities in joint replay common segments

To understand the underlying neuronal firing patterns of joint replays, we compared individual neuronal firing activities during the spatially overlapping segments of joint replays that represented a common arm, between joint replays depicting diverging paths. Take joint CR and CL replays for example: first, we found all the cells that ever fired a spike during the C segment of CR (set 1) or CL (set 2) replays. The size of intersection of the two sets was compared to that of either set to quantify overlap. Next, firing rates during the C segment of each joint replay were calculated for cells belonging to the union of the two sets. Each cell's firing rates in CR and CL replays were compared by using the Kolmogorov-Smirnov two-sample test. Lastly, the distribution of the absolute differences

between cells' mean firing rates in CR and CL was compared to shuffles in which the types of the joint replays were randomized (group sizes were kept the same), also by using the Kolmogorov-Smirnov two-sample test.

Due to the small numbers of joint replays of Rat 2 (see Figure 3.2E) we only used its CR and RL replays in the analyses of this section.

3.2.3 Directionality of replay

Directional place fields were calculated using spike and position data from only inbound or only outbound laps, for each arm. Joint probabilities estimated over both position and direction ((Davidson *et al.*, 2009); time bin = 10 ms) were computed for all identified replays. Two variables were calculated to quantify directionality by using joint probabilities within the corresponding trajectory-specific subregions.

The first variable 'directional', defined by $\frac{1}{M}\sum_{i=1}^{M}\frac{abs(\sum_{j=1}^{N} w1_{ij} - \sum_{j=1}^{N} w2_{ij})}{\sum_{j=1}^{N} w1_{ij} + \sum_{j=1}^{N} w2_{ij}}$ where $w1_{ij}$ and $w2_{ij}$ are the joint probabilities of the inbound and outbound directions of pixel (i, j), measures on average how directional a replay is during each of its time bins. It has a range of 0 - 1, with 0 indicating totally not directional and 1 indicating totally directional. Replays with values larger than 0.3 were considered directional, otherwise they were considered non-directional. The threshold is fixed so that it is independent of the data (same below).

For a replay determined to be directional, the second variable 'bias', defined by $\frac{\sum_{i=1}^{M}\sum_{j=1}^{N} w1_{ij} - \sum_{i=1}^{M}\sum_{j=1}^{N} w2_{ij}}{\sum_{i=1}^{M}\sum_{j=1}^{N} w1_{ij} + \sum_{i=1}^{M}\sum_{j=1}^{N} w2_{ij}}$, was then used to measure if this replay as a whole was consistently biased towards representing either direction. It has a range of -1 to 1, with -1 indicating pure representation of the outbound direction and 1 indicating pure representation of the inbound direction. Replays with values larger than 0.3 were considered to have stronger representations of the inbound direction over the outbound direction; smaller than -0.3 to have stronger representations of the outbound direction over the inbound direction; between -0.3 and 0.3 to have mixed representations of both directions.

Finally, replays were determined to be forward if 'bias' and motion were in the same direction, reverse if 'bias' and motion were in opposite directions and mixed if 'bias' was mixed. For joint replays, directionalities of their two segments were separately determined using joint probabilities within the two corresponding subregions.

3.2.4 Ripple and multi-unit activity analyses

Ripple amplitude was calculated as in (Davidson *et al.*, 2009) with minor changes. We filtered the LFP signal from each selected channel in the ripple band (150-250 Hz), and Hilbert-transformed the filtered signal to compute its envelope as the absolute value of the transformation. The mean envelope averaged across all selected tetrodes (15, 13, and 13 out of 19 tetrodes for rat 1, 2, 3) was smoothed with a Gaussian window (SD = 8 ms)

to represent a continuous mean ripple amplitude. Individual ripples were also detected as local peaks in the ripple amplitude curve over 2.5 standard deviations above the mean, which were both calculated across all stopping periods. We defined the time point at which replay 'passes' the choice point as the mean of inner boundaries of the two corresponding single-arm trajectory-specific subregions. Ripple amplitude trace associated with each joint replay was aligned to this time point to compare ripple amplitude between choice point representation and representations of the preceding and following arms across all joint replays. Multi-unit spikes were defined as all recorded spikes whose largest amplitudes across tetrode channels were larger than 100 μV. Multi-unit spike density was smoothed across 10 ms bins (Gaussian filter, SD = 6 ms).

3.3 Results

Multi-tetrode recordings in the dorsal CA1 area of the hippocampus were conducted in three rats that were exploring the Y maze for the first time. Rats were allowed free exploration and were rewarded with chocolate milk at arm ends according to a spatial alternation rule (see Chapter 2 section 2.1). Putative CA1 pyramidal single units were identified, and their place fields were computed. Only pyramidal cells with peak in-field firing rates exceeding 1 Hz (88 from rat 1, 67 from rat 2, 58 from rat 3) were used in the following analyses.

3.3.1 Abundant joint replays spanning each two connecting arms were identified

To detect hippocampal replay, we first identified candidate events (mean duration 154.6 ms) as transient increases in spike density across all cells, occurring during stopping periods restricted to the three reward areas. A Bayesian decoding algorithm (Davidson *et al.*, 2009) was used to estimate posterior probabilities of position during candidate events. Based on posterior probabilities, candidate events were segmented in position and time, into trajectory-specific subregions (Figure 2.3). Within each subregion, replays were defined as events with a high correlation between position and time, using a weighted correlation method with posterior probabilities as weights. We found large numbers of joint replays in all three animals, which extended across pairs of arms (C ↔ R, C ↔ L and R ↔ L, referred to as CR, CL and RL; rat 1: $N = 164$, rat 2: $N = 32$, rat 3: $N = 66$; see examples in Figures 3.2B-D). These joint replays were readily identified after just the first few running laps across arms and then consistently throughout the recording sessions (see timepoints of example replays in Figure 3.2A).

The significance of replay was evaluated by applying the replay-identification method to shuffled data in which each cell's individual spike train and place field structure were preserved, but the spatial relationship between different cells was disrupted, by circularly shifting the place field of each cell independently by a random number of position bins. For each rat, each type of joint replay was highly significant in number as compared to shuffles (Monte Carlo $p < 0.001$, except for CL of rat 2: $p = 0.025$ and CL of rat 3: $p = 0.002$; Figure 3.2E).

We also observed large numbers of replays representing single arms (Rat 1: $N = 593$, Rat 2: $N = 355$, Rat 3: $N = 203$). However, it is possible that many single-arm replays were partial joint replays where one of the arms was below detection threshold. In support of this, the fraction of spike density events occupied by single-arm replays (ratio of trajectory-specific subregion duration to candidate event duration for each replay) was significantly lower than for joint replays (Figure 3.2F). We therefore focused on joint replays in the following analyses, also for the additional reason that the Y maze structure – the joining of three arms – could only be reflected in the joint replays.

3.3.2 Multiple trajectories were replayed in the same stopping period

Further analyses of replay content revealed that across all stopping periods of the three animals, 90.8 ± 2.4% of the joint replays started from the current arm, confirming the initiation bias that has been reported (Foster & Wilson, 2006; Davidson *et al.*, 2009). Previous reports of replay on a linear track demonstrated that each stopping period was associated with multiple replay events of the same trajectory (Foster & Wilson, 2006). This was interpreted as efficient use of experience. Here we likewise found that individual stopping periods yielded multiple replay events (2.0 ± 0.3 joint replays, and 8.9 ± 1.5 single-arm replays). However, in contrast to the linear track, we observed that on the Y maze, individual stopping periods were associated with multiple replays depicting different trajectories. A large fraction of stopping periods which exhibited joint replay contained replay of multiple different trajectories (38.1%). Indeed, for stopping periods exhibiting joint replay, on average 1.5 ± 0.1 types of joint-arm trajectory (from a

range of 1-3) were represented (see Figure 3.2A). Thus, stopping periods were associated with replay of more than one experience.

3.3.3 Neuronal sequences were bifurcated

While the use of position estimation allowed the information content (*i.e.* trajectory) of replay sequences to be decoded, we further wished to identify the basis of this information content in the responses of individual neurons. In particular, we considered two models that might have accounted for the joint replays we observed. Joint replays could have been encoded using independent populations of neurons (Figure 3.3A), thus the underlying neuronal sequences would be linear, which would in essence be the same neuronal sequences encoding independent linear tracks. Alternatively, common arms of joint replays could have been encoded by the same cells (Figure 3.3B), thus the underlying neuronal sequences would be bifurcated, truly encoding the forked Y maze structure.

For each pair of joint replays proceeding from each arm, the cells which fired during the common segment were almost identical: on average 93.6 ± 2.2% of the cells which fired in one replay also fired in the other. Furthermore, these populations did not differ in firing rate between the two replays. For example, Figure 3.3C shows cells from Rat 1 which participated in firing during the C segments of CR or CL replays. Despite the wide range of firing rates among different cells, each individual cell had almost identical firing rates between CR and CL replays (the almost complete overlap between blue and magenta curves). Across all three rats, an average of 98.0 ± 0.5% of the participating cells (which were 94.9 ± 1.7% of all cells) had no significant difference between their

firing rates during the common segments ($p > 0.05$, Kolmogorov-Smirnov two-sample test). Finally, the distributions of absolute differences in mean firing rate between the two replays were not significantly different from those of shuffles in which replay type was randomized ($p > 0.10$ for all comparisons, Kolmogorov-Smirnov two-sample test; Figures 3.3D-F). These results demonstrate that the same ensemble of cells fired during the common arm of overlapping joint replays with equal firing rates, as if they did not distinguish between the two types of replay, implying that joint replays reflected, at the neuronal level, the bifurcating spatial structure of the maze.

3.3.4 Replays were highly directional

We next asked whether directionality (Figure 3.4A) was encoded by replay and whether it might reflect the structure of the Y maze. Directional place fields were calculated and were used to compute joint posterior probabilities over both position and direction (Davidson *et al.*, 2009), for the already identified replays. The directionality of a replay was quantified using two scores. 'Directional' measured the extent to which the replay tended to be directional during each time bin regardless of which direction was preferred, on a scale of 0 - 1. 'Bias' measured the extent to which a 'directional' replay as a whole favored one direction over the other, on a scale of -1 (outbound) to 1 (inbound). We further compared 'bias' with the direction of motion of replay to categorize replays as either forward ('bias' and motion in the same direction) or reverse ('bias' and motion in opposite directions). Across all three rats, the overwhelming majority of replay sequences (97.7%, including single-arm replays and the component segments of joint replays) had a 'directional' score larger than 0.3. This threshold corresponds to a divergence between the marginal probabilities in either direction such that the probability in one direction was

almost double that in the other (0.65 to 0.35). In fact the mean 'directional' score was 0.62 ± 0.00, which corresponds to a four-fold difference in marginal probabilities (0.81 to 0.19). Thus, replays were highly directional.

We then asked whether the components of joint replays exhibited the same 'bias'. Strikingly, while joint replays exhibited various combinations of 'bias', only 8.0% were either consistently reverse (a reverse sequence of the outbound direction followed by a reverse sequence of the inbound direction, 4.6%, see example in Figure 3.4B), or consistently forward (a forward sequence of the inbound direction followed by a forward sequence of the outbound direction, 3.4%, Figure 3.4C). By contrast, 31.3% of joint replays were composed of segments with opposing biases (such as reverse in the outbound direction followed by forward in the outbound direction, Figure 3.4D). Thus, a large fraction of joint replays switched directionality when 'passing' the junctions of the two represented arms, implying the encoding of the choice point location in replay directionality.

We then asked whether joint replays with opposing biases displayed random combinations or whether instead they obeyed an organizing principle. Strikingly, a far greater fraction of replays was reverse followed by forward (30.5%) than forward followed by reverse (0.8%). Comparing different directionalities for the joint replay segments separately, we found that consistently across stopping periods throughout a session, the first segment tended to be reverse (Figure 3.4F, upper panel) and the second segment tended to be forward (Figure 3.4F, lower panel). This consistency was

maintained across replays initiated in different arms (Figure 3.4F, overbar). This pattern of organization was consistent across the three animals. That is, for each of the three rats it was found that first segments were significantly more reverse than forward ($p < 10^{-4}$ in each rat, Figure 3.4G upper panel) whereas second segments were significantly more forward than reverse ($p < 0.001$ in each rat, Figure 3.4G lower panel). Given the bias for replay to start from the current location and proceed along multiple trajectories, these data suggest replays of the most immediate behavior were mostly reverse, while more diversified and distant replays were mostly forward.

3.3.5 Ripples were specifically associated with arms during joint replays

In a ten-meter long linear track, (Davidson *et al.*, 2009) observed extended replays covering several meters of the track, which were associated with multiple ripple events. Their findings suggested that replays in a large environment were not only extended in duration but furthermore composed of discrete, shorter sub-events. Considering the Y maze as a relatively large environment consisting of spatially distinct segments (the three arms), we wondered whether replay sequences would be associated with multiple ripple sub-events, and whether these events would exhibit a correspondence with the maze structure. Indeed, a majority of joint replays (79.5%) were accompanied by more than one ripple event (median = 2, Figure 3.5). Moreover, joint replays representing the longer CL and RL trajectories were significantly longer and contained significantly more ripples than those representing the shorter CR trajectory (Mean duration: CR = 193.2 ± 3.7 ms, as compared to CL = 234.9 ± 13.7 ms, $t(200) = -4.1$, $p < 10^{-4}$, and RL = 236.8 ± 7.4 ms, $t(227) = -5.7$, $p < 10^{-7}$; Mean ripple number: CR = 2.2 ± 0.1, as compared to CL = 2.6 ± 0.2, $t(200) = -1.8$, $p = 0.068$, and RL = 2.7 ± 0.2, $t(227) = -2.9$, $p = 0.004$, two-sided two-

sample t tests), although not by 1.5 times as the physical joint-arm lengths were. Each type of joint replay also exhibited a positive linear relationship between replay duration and associated ripple number (Linear regression: CR: $R^2 = 0.17$, 9.0 ripples/s, CL: $R^2 = 0.22$, 7.0 ripples/s, RL: $R^2 = 0.33$, 11.9 ripples/s, $p < 0.01$ for each replay type; compare to 9.9 ripples/s in (Davidson *et al.*, 2009)).

We then examined the relationship between ripples and the maze arms depicted in the associated replay sequences. Figures 3.6A-C show example joint replays of each type along with underlying unit activities and accompanying LFP. It can be seen in the raw LFP recordings that 1-2 ripple events occurred during the replay of each individual arm, but ripples did not straddle the choice point. We calculated ripple amplitude as in (Davidson *et al.*, 2009) as a single trace averaging ripple activities across selected tetrodes, and observed similarly 1-2 peaks (corresponding to discrete ripple events) during individual arm representations, together with low ripple amplitude at choice point representations. We then aligned the ripple amplitude trace of each joint replay to the time point when choice point was represented, around which the mean traces across all CL or RL replays also showed 'dips' in between two broad peaks (Mean ratio of ripple amplitude at choice point to averaged amplitude between highest peak on either side of choice point: CL = 0.64 ± 0.04, RL = 0.64 ± 0.03; Figures 3.6E,F,H,I, offset of dips from 0 ms most likely due to inaccuracies in 'choice point passing time' calculations). Interestingly, the 'dip' in the mean CR trace was very small (choice point – to – peak average ratio = 0.74 ± 0.02, Figures 3.6D,G), suggesting that the effect was most prominent for replays representing longer trajectories, that extend for longer durations

and contain more ripples. Furthermore, this effect was not simply due to weaker place-field representation at the choice point. By computing two-dimensional place fields we compared the mean firing rate across all pixels located within choice-point area (≤ 10cm along linearized directions to track center), with the mean firing rate across all pixels within track arms (>15cm along linearized directions to track center), across all cells. We found that place-field representation at the choice point was similar to, or marginally stronger than, the representation at arm portions of the Y maze: Rat 1: choice-point = 1.72 ± 0.22 Hz, track-arms = 1.33 ± 0.14 Hz, $t(174) = 1.5$, $p = 0.14$; Rat 2: choice-point = 1.83 ± 0.34 Hz, track-arms = 1.12 ± 0.13 Hz, $t(132) = 1.9$, $p = 0.055$; Rat 3: choice-point = 1.67 ± 0.24 Hz, track-arms = 1.34 ± 0.14 Hz, $t(114) = 1.2$, $p = 0.23$ (unpaired two-sided two-sample t tests). Thus, in addition to demonstrating that extended joint replays were composed of multiple discrete sub-events, we made the observation that these sub-events clustered into representations of entire single arms, rather than of random portions of the joint-arms.

3.3.6 Joint replays were detected after little experience

We further asked, given that joint replays with environment-specific structure occurred during the first exposure to the environment, how rapidly within the session can such replay be detected? To address this question, we determined the stopping periods by which joint replays reached significant numbers, by counting the cumulative number of each type of joint replay for each stopping period, in original and shuffled data. We then counted the number of experiences of a replay before the first significant stopping period for that replay. For example, for Rat 1, all three types of joint replay rapidly outgrew shuffles in numbers (Figures 3.7B-D) and reached significant numbers after 2 - 4

experiences of the corresponding joint arms (Figure 3.7A). This pattern was replicated for every joint replay type, in each animal independently. Each animal acquired at least one of the joint replays after only 2 laps on the track (Figures 3.7B-J). Across all animals, an average of 3.3 ± 0.4 laps on corresponding joint-arms were experienced before the first significant stopping periods.

3.4 Discussion

3.4.1 Y maze structure was captured by individual neuron and population activities

In this study, we asked whether and how hippocampal place-cell sequences would reflect the topological structure of an environment of unpredictable shape, with the hypothesis that navigationally useful sequences should capture this structure. We found that patterns of replay developed during the first exposure to a nonlinear environment that matched the sequential structure of the environment. This structure included unique elements such as bifurcated paths, and unequal lengths of the track arms. Most importantly, this nonlinear structure was captured at the level of the individual neurons. Spatially overlapping episodes (*i.e.* the common part of pairs of joint arm traversals) were not replayed by independent populations of neurons, but by the same neurons with the same firing rates. Hence, the neuronal activities appear to be effectively "stitched together" in a manner reflecting the shape of the maze. Since replay structure may be determined by the functional connectivity pattern among recruited neurons, our result implies that different experiences of the track were encoded not by drawing random neuronal sequences from the network, but rather in such a way that each novel experience activates the

participation of a neuronal sequence (with new neurons and new connections) that match the spatial relationship between the novel experience and the familiar portion of the environment. Because the structure of the maze was unpredictable, these findings suggest that the neural network mechanisms responsible for generating these place-cell sequences involve learning.

The common coding scheme for spatially overlapping replays may have functional implications. Even though the animals traversed one joint-arm trajectory at a time, the separate running experiences were integrated in the brain so as to reflect the correct connectivity between the three track arms. This observed property of replay implies the construction of a map-like hippocampal representation of the navigational environment as a whole, which importantly enables the 'prediction of what leads to what' (O'Keefe & Nadel, 1978) and consequently flexible calculations of efficient routes between any two locations within the environment. This form of representation may support the generation of novel routes, such as short cuts, as well as appropriate generalization in the face of changes to the environment *e.g.* effective detours to avoid novel obstacles. Such a scheme has clear advantages for navigation over the unintegrated representation of separate experiences, as would the case if bifurcated paths were encoded by different populations of neurons, since this scheme would only support the selection of paths from the limited repertoire of encoded paths gained through direct experience. This observation made in the relatively simple Y-maze may imply a basic coding scheme for more generalized environments, whereby the hippocampus encodes the complete spatial structure as opposed to separate running experiences.

Additionally, we found that joint replays were accompanied by multiple ripple events, confirming a recent finding that extended replays may be composed of discrete sub-events (Davidson *et al.*, 2009). Moreover, ripple occurrence was confined within the boundaries of joint replay segments that represented individual arms, which suggested that the precise times at which ripples were generated during replay were not random. Instead, one or more sub-events were closely clustered to represent linear components of the environment, while longer intervals between clusters accurately signaled the location of the arm intersection, again matching the spatial structure of the Y maze. Furthermore, the difference in arm lengths was also reflected by replay, in that physically longer trajectories (CL and RL) were represented by replays longer in duration, and correspondingly larger numbers of ripple events. The ratios of replay duration and ripple number between CL/RL replays and CR replays did not exactly match the ratios of track lengths (1.2 compared to 1.5), but this might have been due to systematic bias in the measurement of longer sequences when recording from limited numbers of hippocampal neurons.

3.4.2 Implications of joint replay directionality

The directionality of replay sequences, and the existence of both forward and reverse sequences, have been reported previously for linear tracks and linear trajectories (Lee & Wilson, 2002; Foster & Wilson, 2006; Csicsvari *et al.*, 2007; Diba & Buzsaki, 2007; Davidson *et al.*, 2009). Here, we further show that replays of the linear pieces of a more complex environment are also overwhelmingly directional. Previous reports of replay on an extended track indicated that replays did not always represent a consistent

directionality, but could flip between forward and reverse (Davidson *et al.*, 2009). Here we also see direction flipping, which in fact predominated among joint replays, with the additional finding that replay tended to flip direction around the choice point, supporting the notion that replay captured the unique structure of the environment. We further found that rather than the combination of forward and reverse components occurring at random, there is a distinct organizational pattern such that first segments of joint replays tended to be reverse, and second segments of joint replays tended to be forward. This finding combines in a fascinating way with two other findings in this task. First, we find that replay tends to start in the current arm. Second, we find that successive replays during single stopping periods can proceed along different trajectories. Integrating across these results, we can make the observation that joint replays tended to begin on the current arm and proceed in reverse order, before switching at the choice point to proceed along either of the two other arms in forward order. This organization suggests that reverse and forward replays may have different functions, with reverse replay representing a rewind of the immediate past, and forward replay representing the exploration of alternative futures, perhaps for the purposes of planning future behavioral trajectories. It is important to distinguish this classification of forward and reverse based on the directional tuning of place fields during bidirectional running (*i.e.* replays extending from point A to point B, or from point B to point A, can both be either reverse or forward), as used in the original report of reverse replay (Foster & Wilson, 2006), from an alternative classification that has been used, based on whether replay extends along the same unidirectional running path imposed by the task, or the opposite, never experienced running direction (*i.e.*

replays extending from point A to point B are defined as forward, replays extending from point B to point A are defined as reverse) (Gupta *et al.*, 2010).

3.4.3 Rapid occurrence of joint replays

Recurrent networks in the hippocampus have highly modifiable synapses which are likely to undergo rapid synaptic plasticity during exploration (Buzsaki, 1989; Wilson & McNaughton, 1994; Martin *et al.*, 2000; O'Neill *et al.*, 2010), giving rise to rapidly reconfigured hippocampal circuits. Several computational models of the hippocampus have established the feasibility of using experience-dependent synaptic plasticity to acquire novel sequences (Jensen & Lisman, 1996; Levy, 1996; Leibold & Kempter, 2006; Molter *et al.*, 2007; Koene & Hasselmo, 2008), in some cases after a single trial of behavioral experience. Consistent with these models, we found that joint replays were detected in significant numbers after very few trials of experience. For several reasons, these numbers of trials before significant replay was detected are likely to be an overestimate. First, stopping period durations were at the discretion of the animal, and longer stopping periods would have increased the probability of observing replay at earlier timepoints. Second, many single-arm replays may have been in fact joint replays for which one arm failed to pass detection threshold (Figure 3.2F), because of inherent experimental limitations on our ability to measure replay, given that the number of neurons recorded represents only a tiny fraction of the total network. Rapid learning is a prominent feature of hippocampally dependent learning (Morris, 2001), and so the rapid learning of replay sequences may play a fundamental role in hippocampal function.

3.4.4 The phenomenon of 'preplay'

The standard interpretation of replay is that it represents a form of sequence memory, which may require synaptic plasticity to become established (Molter *et al.*, 2007; Koene & Hasselmo, 2008; O'Neill *et al.*, 2010). However, it was recently reported that neuronal sequences recorded prior to an experience matched the sequential order in which neurons responded during that experience (Dragoi & Tonegawa, 2011). These "preplay" sequences appeared to be indistinguishable in form from replay sequences, for example, they were similarly temporally compressed. The interpretation of this result was that, because experience is temporally linear, the hippocampus might utilize preexisting linear sequences to schedule the recruitment of place cells during subsequent behavioral episodes, in a manner analogous to laying down movies on videotape. However, although it is still an open question whether what is found from pre-sleep recordings are directly applicable to awake replays, which occur in a very different behavioral state, a remarkable corollary of this result is that all replay sequences observed subsequent to experience might in fact reflect pre-established sequences. We would like to distinguish our study from that of (Dragoi & Tonegawa, 2011) in the following arguments: First, the demonstration of preplay was in a task with linear structure, such that a pre-existing temporal order might control the subsequent recruitment of place cells. By contrast, we used a running maze with a forked structure, in which no linear order can be mapped continuously onto the spatial layout. Secondly, although the preplay study was recently repeated in rats (Dragoi & Tonegawa, 2013), some previous rat studies failed to observe preplay (Lee & Wilson, 2002; Foster & Wilson, 2006) which used similar sequence detection methods to (Dragoi & Tonegawa, 2011). To determine whether nonlinear

replays observed in complex environments are generated by pre-existing sequences or novel neuronal sequences formed from rapid reconfiguration of the hippocampal network, future research is required in detailed analyses of data recorded prior to any experience in complex environments in rats. Preliminary results from our pre-behavioral sleep recordings show that *zero* joint replay of any kind was detected from pre-sleep sessions of three rats, while all three types of joint replay were independently significant in numbers for each rat during run sessions ($p < 0.03$, Rat 2, 3, & additional Rat N); single-arm sequences were detected in pre-sleep sessions, which were insignificant in numbers as determined by using our place-field modular shuffle method ($p > 0.09$ for all rats) – although this result is confounded by the uncertainties in measuring single-arm sequences (Figure 3.2F). When recorded sufficient post-behavioral sleep data (Rat N), we found significant joint replays of all types (CR: N = 20, $p = 4 \times 10^{-4}$, CL: N = 4, $p = 0.006$, RL: N = 5, $p = 0.007$) in the post-sleep session. It is important to note that pre-sleep single-arm sequences are visually much lower in quality – much shorter in duration and more fragmented, with big jumps between positions represented with high probabilities – which are in clear contrast to run and post-sleep single-arm replays depicting continuous and extended trajectories with smooth transitions between adjacent locations (Figure 3.8). Post-sleep joint replays also exhibited high qualities in close approximation to run joint replays (Figure 3.9). Thus, our results question the existence of preplays matching trajectories experienced in a complex spatial environment; we also demonstrated that pre-existing sequences matching linear components of a complex environment, although detectable, or maybe even significant in numbers by using other significance-testing methods or experimental paradigms, are drastically different in

quality as compared to sequences detected after experience, which may imply weak synaptic connections or lower numbers of recruited neurons in the pre-existing place-cell sequences. The considerable improvement in quality in run and post-sleep replays, on the other hand, suggests that sequences were indeed modified by experience to more accurately represent the environment, if not established anew by experience. In general, however, it is puzzling whether the space of 'spatial complexity' needs to be exhausted in order to determine whether pre-existing sequences exist for all possible spatial structures; also, the essential question is whether the sequences are already encoded in the hippocampal network, not whether they are expressed as preplay events, since it is possible that certain sequences are not preplayed but stay latent in the hippocampal network at the time of recording. Nonetheless, we acknowledge the fact that the question of whether replay is the result of learning still remains unanswered.

Finally, we showed that while sequences can be encoded rapidly, they are also rapidly fit into a structure which captures the sequential spatial structure of the environment. Thus, while hippocampal replay may be formed out of the experience of individual episodes, its adaptive role may rather lie in the construction of predictive representations to guide future behavior (Wood *et al.*, 1999; Frank *et al.*, 2000; Schacter & Addis, 2007; Pfeiffer & Foster, 2013). Determining the full relationship between hippocampal replay and hippocampally dependent learning, memory, and planning is a key future goal.

Figure 3.1

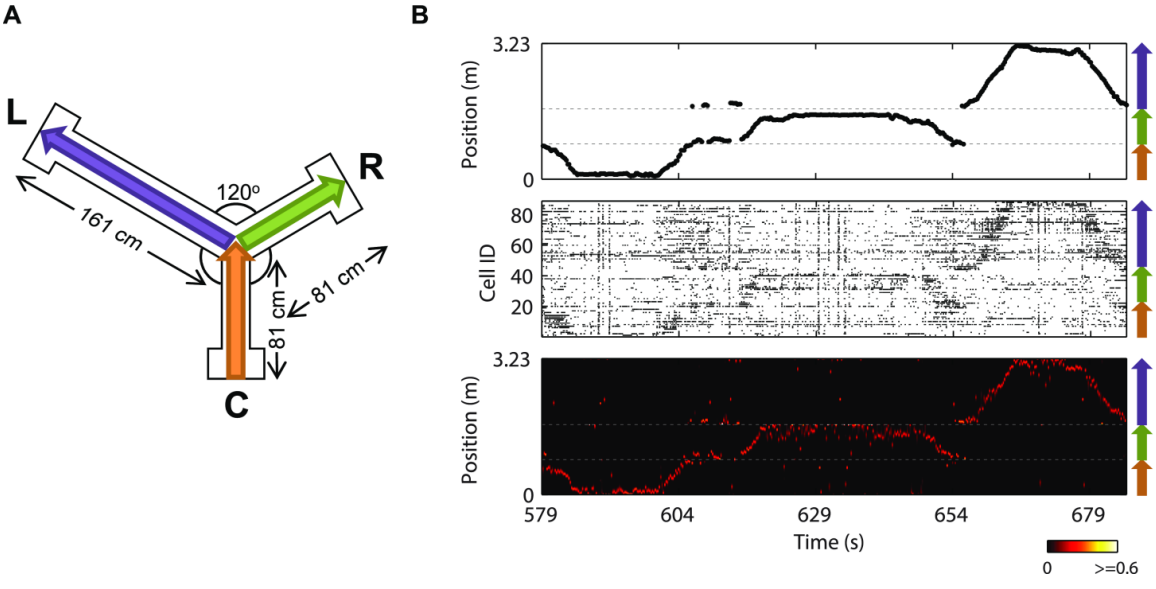

Figure 3.1 Place cell activities in modified Y maze

(A) Modified Y maze. C: central arm, R: right arm, L: left arm.

(B) An example epoch of 106 s of recording. Top: Linearized running trajectory of Rat 1. Horizontal dashed lines indicate arm boundaries. Colored arrows on right indicate arm alignment along linear axis (same below). The rat ran through center → C → center → R → center → L → center. Middle: Simultaneously recorded spike trains from 88 putative place cells, ordered by locations of the cells' peak firing rates on linearized track. Position estimation based on these spikes is shown at bottom, where posterior probabilities of position representations in each 250 ms window were indicated by hot scale.

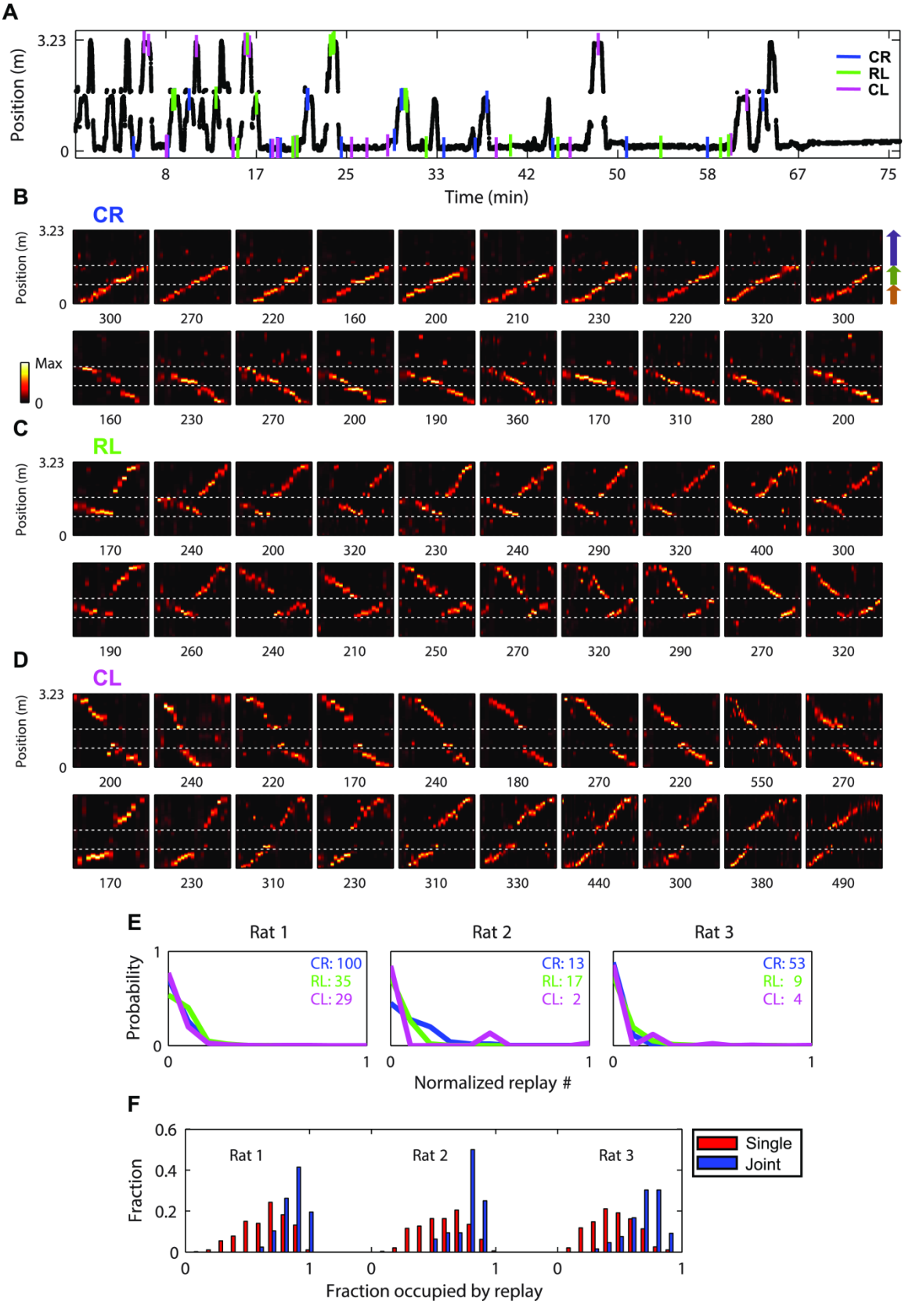
A
Position (m)
3.23
0
CR
RL
CL
8
17
25
33
42
50
58
67
75
Time (min)
B
CR
Position (m)
3.23
0
300
270
220
160
200
210
230
220
320
300
Max
0
160
230
270
200
190
360
170
310
280
200
C
RL
Position (m)
3.23
0
170
240
200
320
230
240
290
320
400
300
190
260
240
210
250
270
320
290
270
320
D
CL
Position (m)
3.23
0
200
240
220
170
240
180
270
220
550
270
170
230
310
230
310
330
440
300
380
490
E
Rat 1
Rat 2
Rat 3
Probability
1
0
CR: 100
RL: 35
CL: 29
CR: 13
RL: 17
CL: 2
CR: 53
RL: 9
CL: 4
0
1
Normalized replay #
F
Fraction
0.6
0.4
0.2
0
Rat 1
Rat 2
Rat 3
Single
Joint
0
1
Fraction occupied by replay

Figure 3.2 Joint replays were detected from neuronal data in significant numbers

(A) Linearized position as a function of time for Rat 1 during first exposure to the modified Y maze. Colored ticks mark when and where example replays in panels B,C,D occurred.

(B,C,D) Examples of identified replay events representing CR, RL, and CL trajectories from a single rat (Rat 1), in which position is decoded from neuronal spike trains in non-overlapping 10 ms bins. Horizontal dashed lines mark arm boundaries. Replays in each row are ordered by the time of occurrence. The duration of each event in ms is shown below each example.

(E) For each pair of joint-arms, the probability of observing the number of identified joint replays by chance is expressed as the distribution of the numbers of replays representing the same joint-arms sampled from 5000 shuffles as fractions of the number of joint replays actually observed (numbers in inset). Each type of replay from each animal was highly significant.

(F) Histograms of fractions of candidate event time windows occupied by single-arm replays and joint replays are plotted for each animal, normalized by the total numbers of replays. Single-arm replays (0.6 ± 0.0 across all rats) occupied significantly smaller fractions of spike density events than joint replays (0.8 ± 0.0 across all rats; Rat 1: $t(755) = -14.6$, $p < 10^{-42}$; Rat 2: $t(385) = -5.8$, $p < 10^{-7}$; Rat 3: $t(267) = -10.1$, $p < 0.02$).

Figure 3.3

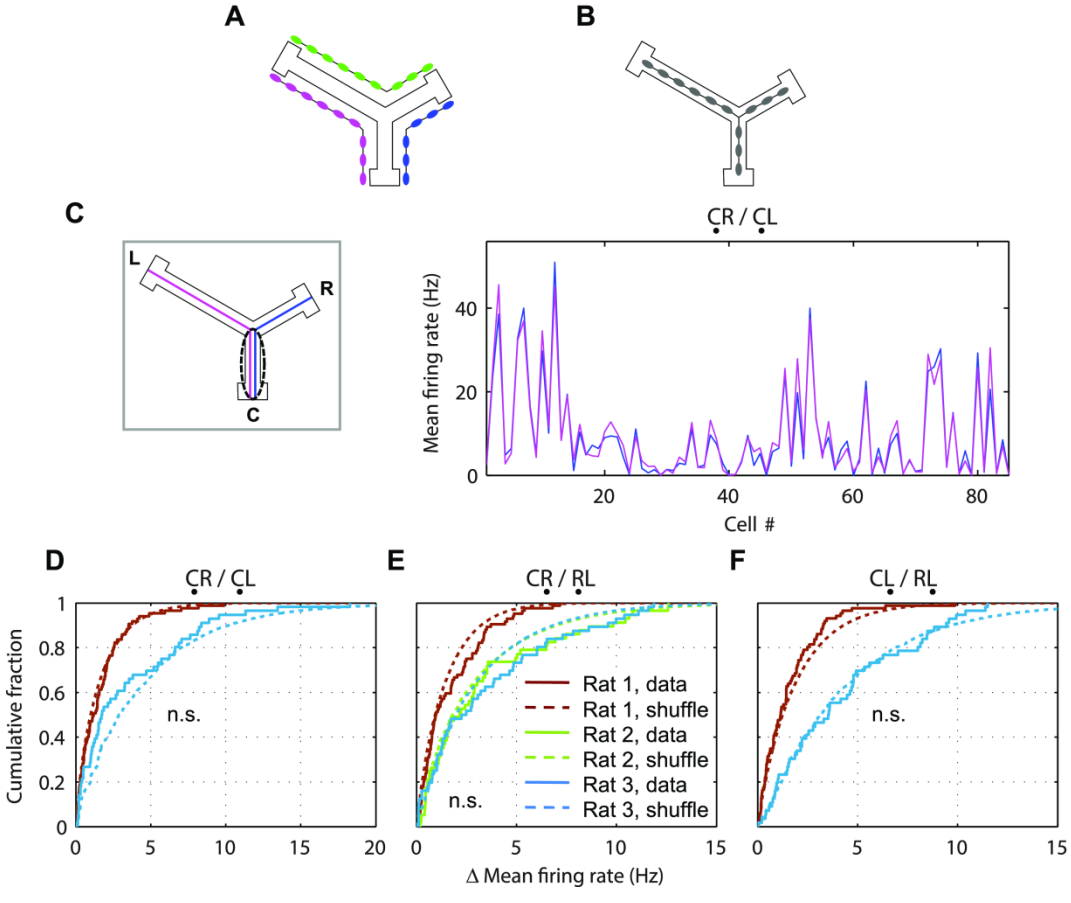

Figure 3.3 The same group of cells fired during common segment of joint replays

(A,B) Two hypotheses of how joint replays might be encoded. (A) Illustrates three independent populations of place cells with three separate sequences of place fields on the Y maze. Each pair of joint-arms is encoded by a separate sequence. (B) Joint replays were generated by a neuronal network which captures the spatial structure of the Y maze. The common segment of each pair of joint replays is generated by two different groups of cells in (A) and the same group of cells in (B).

(C) Mean firing rates of cells from Rat 1 during the common segment C of joint CR (blue) and CL (magenta) replays. The included cells fired at least one spike during the C part of at least one CR or CL replay. Note that firing rates for the two replay types are highly similar across cells.

(D,E,F) Solid curves show cumulative distributions of absolute differences between cells' mean firing rates during the common segments of paired joint replays (*e.g.* the blue and magenta curves in panel C). Dashed curves show distributions calculated from 5000 shuffles in which replay types (*e.g.* CR and CL) were randomized.

Figure 3.4

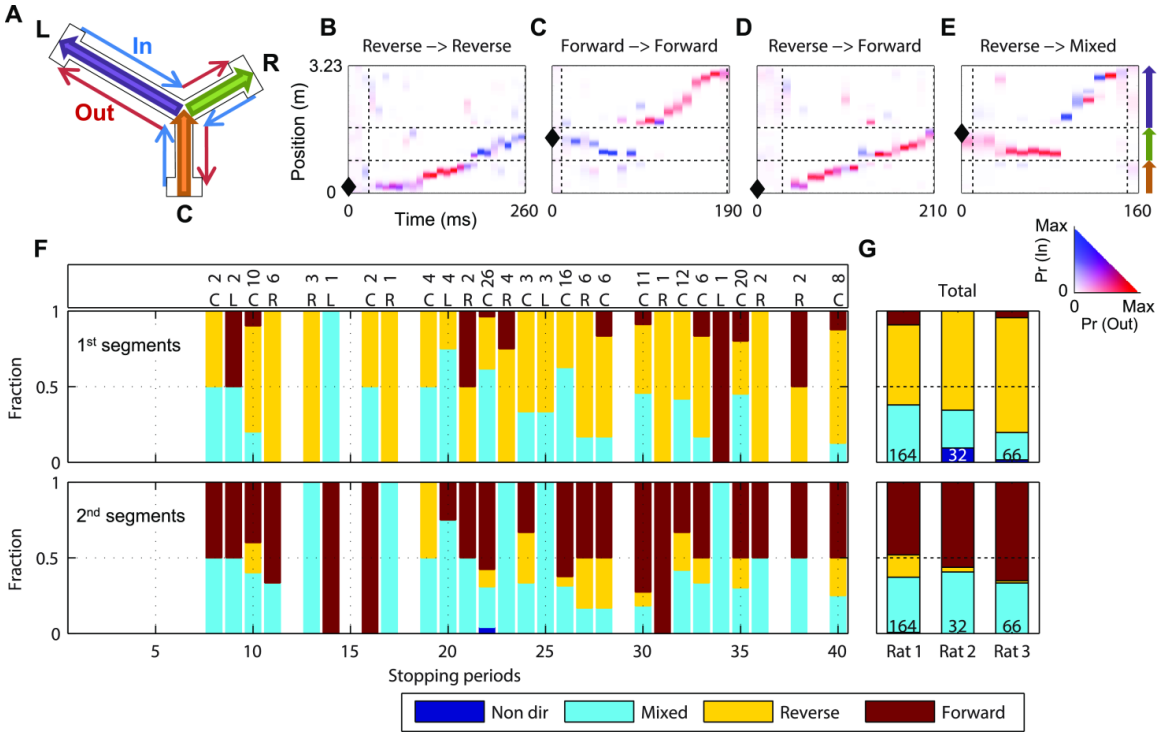

Figure 3.4 Joint replay directionality

(A) The junction of the three arms is the choice point. Running towards choice point is 'inbound', running away 'outbound'.

(B-E) Examples of joint replay with different combinations of directionalities from Rat 1. Horizontal dashed lines indicate arm boundaries. Black diamond shapes mark location of the rat when each replay occurred. Color scale set so that maximally saturated colors correspond to the largest position probability of each replay. (B) A consistent reverse replay of CR. (C) A consistent forward replay of RL. (D) A CR replay with a reverse C

segment followed by a forward R segment. (E) An RL replay with a reverse R segment followed by a mixed L segment.

(F) Each bar shows, for all joint replays with at least one directional segment identified during each stopping period, the percentage of the first segments (upper panel) or the second segments (lower panel) with each directionality type (see legend). Joint replay number and location of each stopping period are shown in the overbar. Data from Rat 1.

(G) Percentages calculated for all stopping periods combined, for the three rats separately. The total number of joint replays (with at least one directional segment) is shown in each bar plot for each rat. For each of the three rats it was found that first segments were significantly more reverse than forward: Rat 1: reverse = 0.58 ± 0.06, forward = 0.13 ± 0.05, t(52)=6.0, $p<10^{-6}$; Rat 2: reverse = 0.67 ± 0.11, forward = 0, t(16)=6.1, $p<10^{-4}$; Rat 3: reverse = 0.77 ± 0.07, forward = 0.05 ± 0.04, t(52)=9.1, $p<10^{-11}$. For each of the three rats it was also found that the second segments were significantly more forward than reverse: Rat 1: reverse = 0.11 ± 0.03, forward = 0.44 ± 0.06, t(52)=-5.2, $p<10^{-5}$; Rat 2: reverse = 0.01 ± 0.01, forward = 0.47 ± 0.11, t(16)=-4.3, $p<10^{-3}$; Rat 3: reverse = 0.00 ± 0.00, forward = 0.63 ± 0.08, t(52)=-7.5, $p < 10^{-9}$.

Figure 3.5

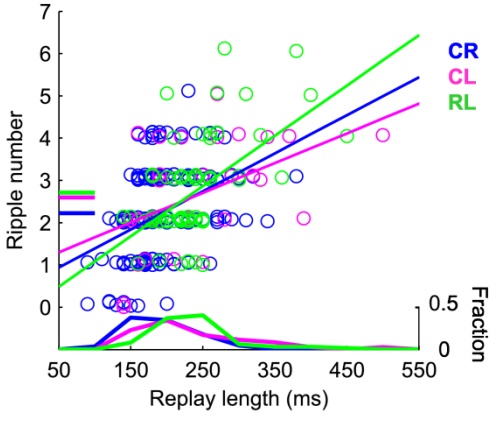

Figure 3.5 Joint replays were associated with multiple ripples

The number of ripples detected during each joint replay (during the joint trajectory-specific subregion) was plotted against the duration (subregion length) of each replay, with each replay type plotted in a different color. For visualization purpose only random noise was added to ripple numbers. Horizontal lines on left indicate mean ripple numbers. Histograms of replay durations are shown at bottom. Diagonal lines: linear regressions based on each replay type.

Figure 3.6

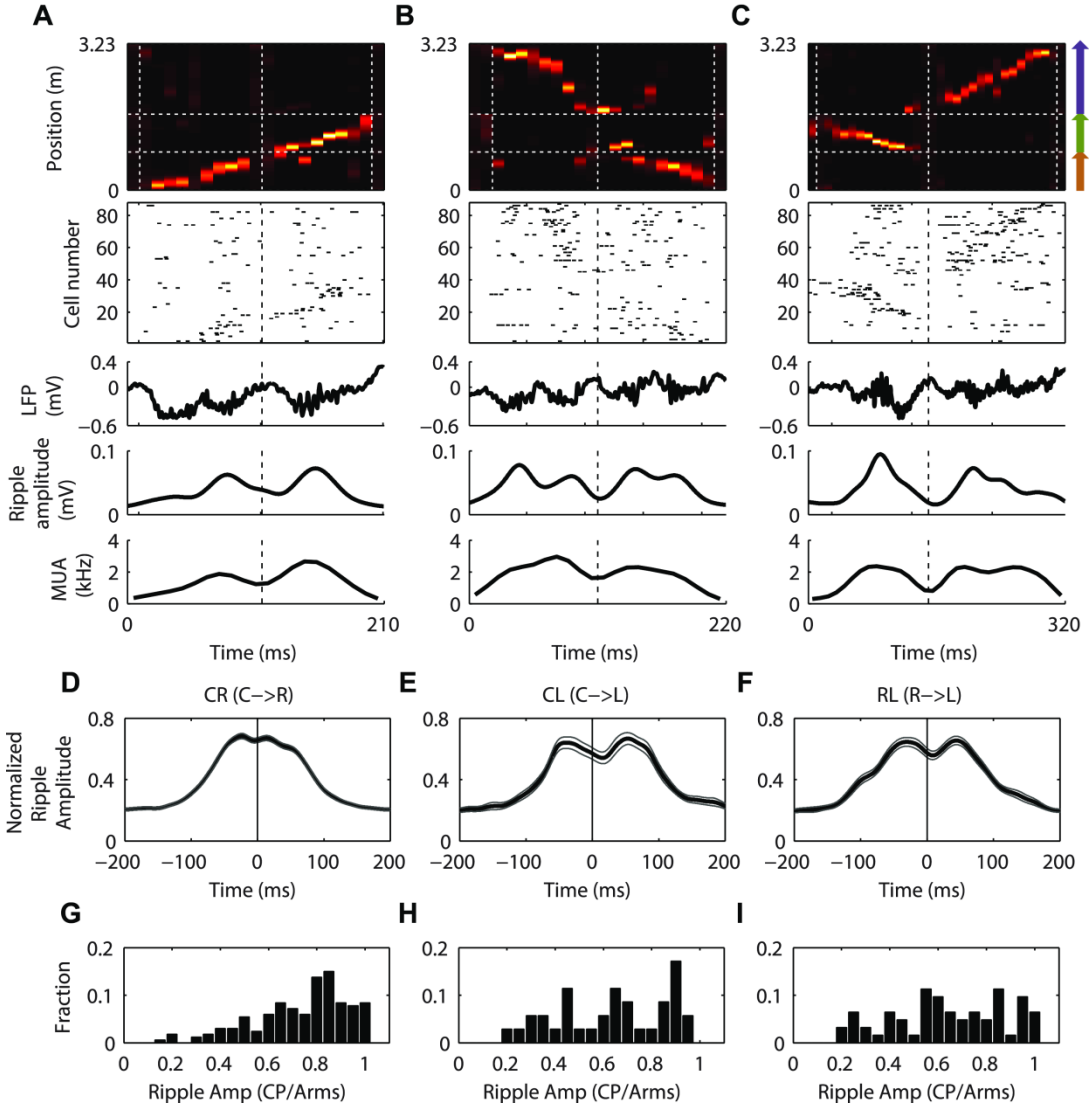

Figure 3.6 Ripples specifically co-occurred with arm representations

(A,B,C) Examples from Rat 1. Top to bottom: decoded joint replays of CR, CL, and RL; place cell spikes during replay with cells ordered by locations of their peak firing rates on linearized track; raw LFP recording from one selected tetrode channel; ripple amplitude;

multi-unit spike density as a function of time. In all panels vertical dashed lines at center indicate the time of choice point representation during replay, which in (B) were moved to left by two bins (20 ms) for illustration purpose solely.

(D,E,F) Ripple amplitude traces (*e.g.* those shown in A,B,C) of all joint replays, each normalized to its own maximum amplitude, were each aligned to the time when choice point was represented during replay (0 ms in each panel, indicated by vertical black lines). They were also reoriented to the same joint-arm directions noted in titles, *e.g.* traces of R → C replays were all flipped around 0 ms. Shown for each replay type are mean ± s.e.m of the resulting traces across all three rats.

(G,H,I) Histograms of ratios of ripple amplitude at 0 ms to mean of peak ripple amplitudes on either side of 0 ms.

Figure 3.7

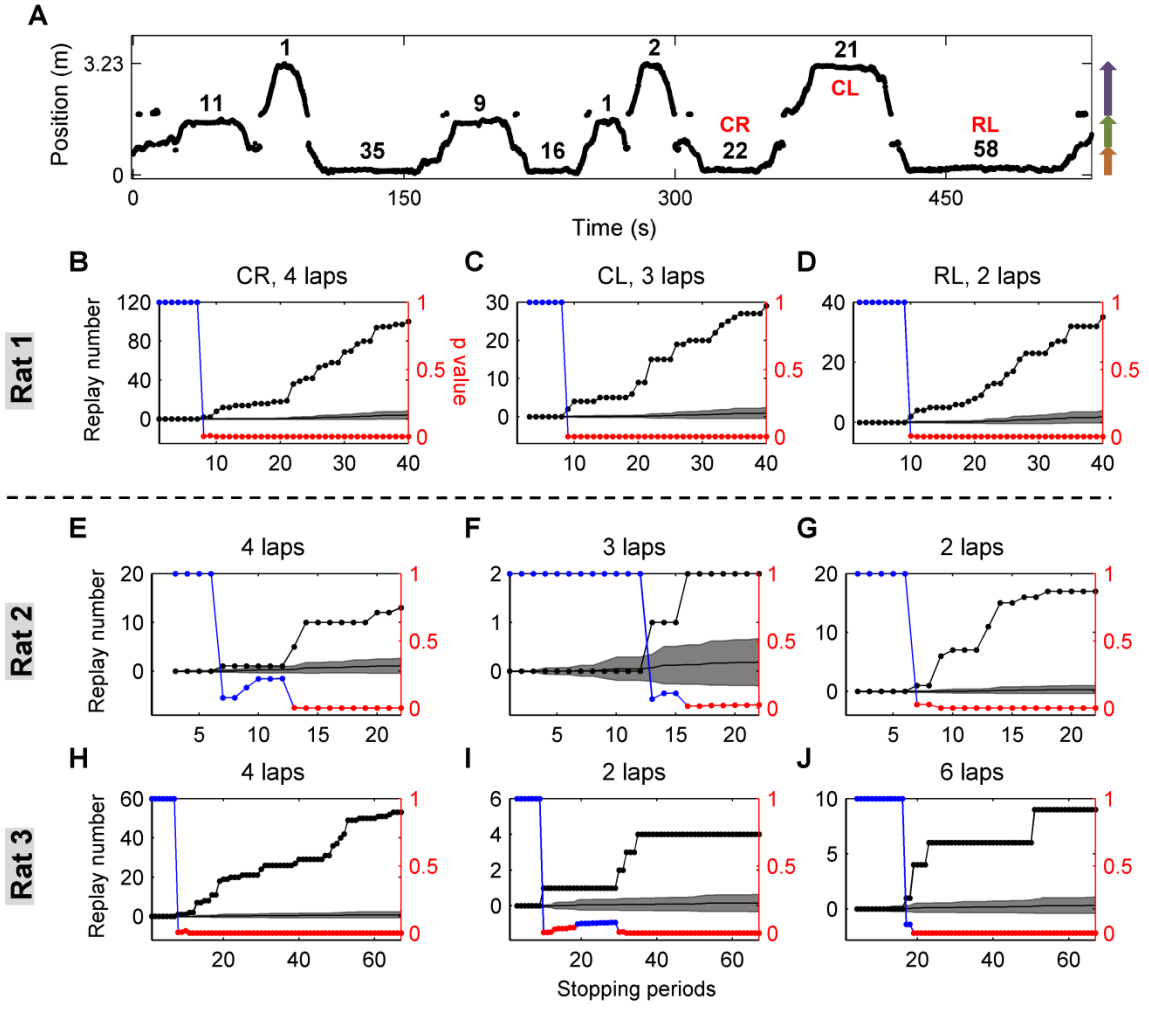

Figure 3.7 Joint replays reached significant numbers rapidly

(A) The first 10 stopping periods of Rat 1 (recorded position). The numbers of candidate events found during each stopping period are noted next to the stopping periods. Red letters indicate the stopping periods by which the noted types of replay first reached significant numbers.

(B,C,D) Each panel demonstrates how the number of observed replays outgrows those counted from shuffles (data from Rat 1). Dotted black lines: cumulative numbers of replays detected from the original data. Gray shadings: mean ± s.d. of cumulative numbers of replays of the same type detected from 5000 sets of shuffled data. Colored dotted lines: Monte Carlo p values of the original cumulative numbers; blue: $p >= 0.05$ (not significant); red: $p < 0.05$ (significant). The numbers of laps on corresponding joint-arms run before the first significant stopping periods are noted in titles.

(E-J) Results for Rats 2 and 3 are shown in (E,F,G) and (H,I,J).

Figure 3.8

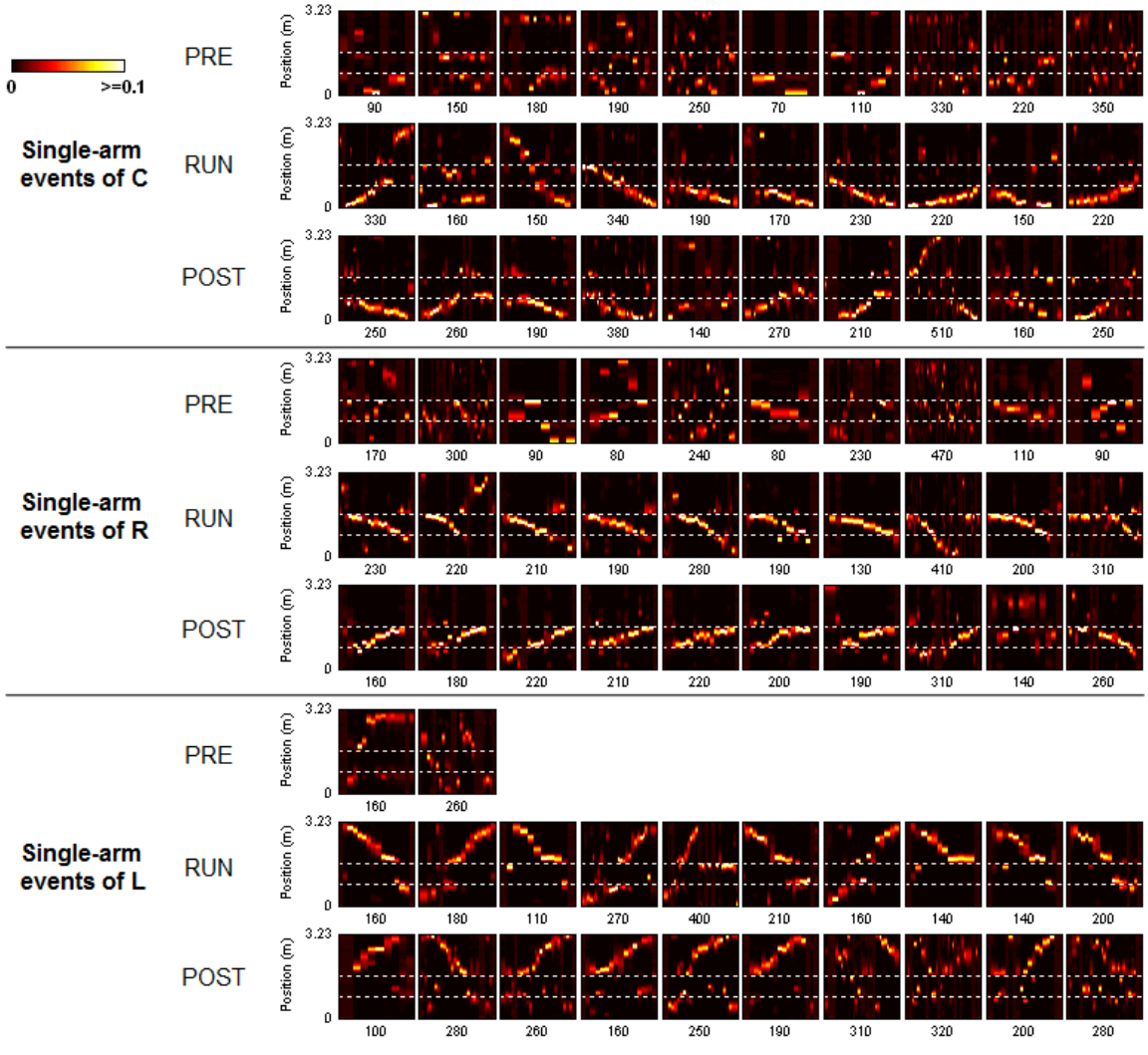

Figure 3.8 Place cell sequences representing single arms identified from pre-sleep, run, post-sleep sessions

For each single-arm representation, ten events with the highest absolute weighted correlation values, or all events if fewer than ten, are plotted for each recording session (pre-sleep: PRE, run: RUN, post-sleep: POST) in the order of high to low absolute

weighted correlations. All events are from a new Rat N and are plotted with the same color scale (see color bar). Position is decoded in non-overlapping 10 ms bins. Horizontal dashed lines mark arm boundaries. The duration of each event in ms is shown below each example.

Figure 3.9

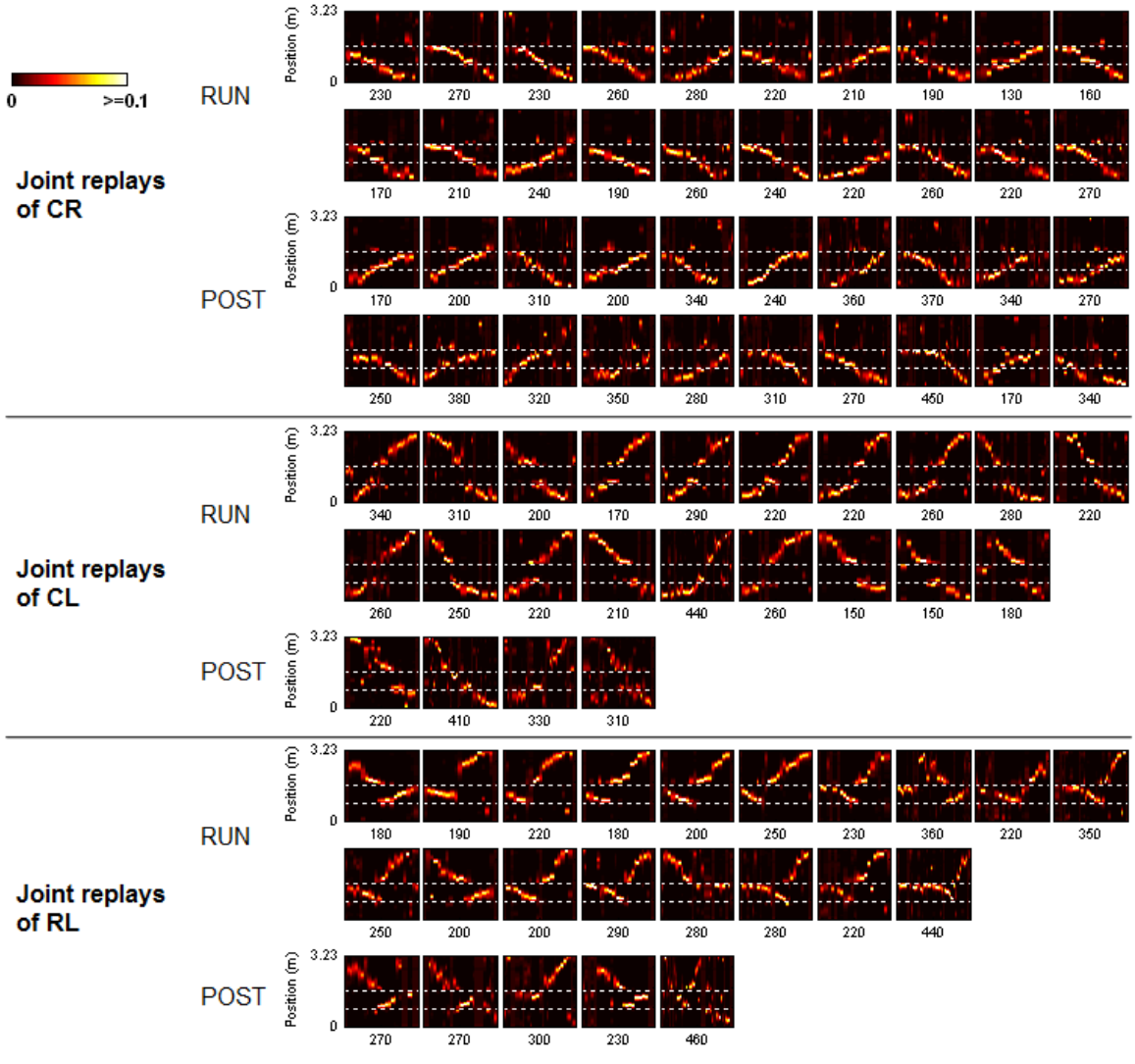

Figure 3.9 Place cell sequences representing joint arms identified from run and post-sleep sessions

For each joint-arm representation, twenty events with the highest absolute weighted correlation values, or all events if fewer than twenty, are plotted for run (RUN) and post-sleep (POST) sessions (zero joint-arm sequence was detected from the pre-sleep session),

in the order of high to low absolute weighted correlations. All events are from a new Rat N and are plotted with the same color scale (see color bar). Position is decoded in non-overlapping 10 ms bins. Horizontal dashed lines mark arm boundaries. The duration of each event in ms is shown below each example.

Chapter 4 Activity changes of medial prefrontal neurons coincident with hippocampal replay events depended on replay representation

The hippocampal replay has been hypothesized to play functional roles in cognitive processes important for guiding behavior, yet experimental data suited to lend support to this hypothesis is still largely lacking. We aimed to provide evidence from a mechanistic point of view, by searching for correlations between hippocampal replay and prefrontal neuronal activities, with the working hypothesis that the existence of such correlations suggests the involvement of hippocampal replay in brain processes that the prefrontal cortex has been well documented to play a major role in. We recorded neuronal activities simultaneously in the CA1 area and the medial prefrontal cortex in rats learning an alternation reward rule while exploring a Y-shaped maze, following procedures described in Chapter 2.

4.1 Quantification methods

Methods for processing the hippocampal recordings as well as for the identification of replay sequences remained the same as those described in Chapter 2, with the only difference that the Bayesian-based position estimates were applied to overlapping 20ms time bins advancing in 10ms increments in the current chapter, instead of the 10ms non-overlapping time bins used in Chapter 3, to increase the accuracy in position estimates and replay identification.

4.1.1 Selection of mPFC single units

Well isolated single units recorded in the medial prefrontal cortex were included in the subsequent analyses if the following criteria were met: 1) mean peak-to-trough spike width > 0.35 ms; 2) fewer than 5% of all spikes occurred within the refractory period (interspike interval < 2 ms); 3) average firing rate over the entire recording session is higher than 0.2 Hz. These criteria were set to ensure exclusion of noisy clusters, units with ultra-low firing activities, and interneurons, selecting a total of 54 putative pyramidal units for the following analyses, with 16 units recorded from Rat 1 Day 4, 11 from R2D2, 13 from R3D1, and 14 from R4D1.

4.1.2 Running direction modulation of mPFC neuronal activities

Recorded positions were projected onto three lines (defined by the experimenter) aligned with the three arms of the Y maze, as was performed for hippocampal place field calculations. For each unidirectional running lap on each arm, occupancy time normalized firing rates during that single lap were calculated for each mPFC neuron in linearized position bins (7.3 – 7.9 cm for rats 1-4), using data from periods with running speed > 5 cm/s. Note that position bins on each arm started from the junction of the three axes to avoid crossing between arms. Subsequently, the firing activities of each individual neuron during each complete unidirectional running-lap from one arm end to another was reconstructed with the firing-rate vectors on the component arms previously separately calculated, which were smoothed across both arms with a Gaussian window (SD = 1 bin) to ensure accuracy of firing-rate estimates around the choice point. The resulting position tuning curve was separated between arms again, such that each

neuron's firing activities during active running, in either the inbound or outbound direction on each arm, could be gathered from all laps with the same arm-direction combination for visualization and statistical analysis.

4.1.3 Medial prefrontal neuronal activities at replay occurrence

To look for consistency in firing patterns of mPFC neurons co-occurring with hippocampal replay sequences, we extracted spikes from each mPFC neuron fired within ± 5 secs of the center time of each replay event (mean over boundaries of the trajectory-specific subregion of the single or joint replay). Each 10-sec epoch of spikes was converted into firing rates in 30-ms bins, which were smoothed with a Gaussian filter with SD = 60 ms. The smoothed firing-rate traces of each mPFC neuron were truncated to 1) within ± 0.75 secs of replay-event centers for display, 2) within ± 0.6 secs of replay-event centers for statistical analysis, and 3) two one-sec long time windows one second prior to and after replay-event centers for baseline firing-rate calculations; the original wider, ± 5 secs time windows were used to eliminate the edge effect of smoothing.

In the initial examination of mPFC activity patterns co-occurred with hippocampal replay events, we compared individual mPFC neuron's firing activities extracted from all single- and joint-arm replay windows to those aligned to the center time-points of high population firing (candidate) events lacking replay structure as determined by our replay identification method. Subsequent comparisons were made between mPFC activities centered on single-arm replays representing different track arms, to study whether the information content of replay affected the firing patterns of mPFC neurons.

4.1.4 Statistical analysis

We mainly used the permutation test for significance estimates because it is 'model-free'. The permutation test does not require assumptions of stochastic models of neuronal firing, or independent firing rates in adjacent time or position bins, or normally distributed firing rates across trials (Steinmetz *et al.*, 2000), which do not often characterize actual neuronal firing activities. The permutation test also allows the freedom of constructing any test statistic that is most relevant to the statistical question, which is calculated for the original data and shuffled data in each permutation. The comparison between the original value and the permutation distribution (each test included 5000 permutations) yields a p value (significance set at $p < 0.05$ in this study). One test statistic we used was the sum of squared differences. For comparisons between two conditions, the mean firing-rate vector averaged across all trials belonging to one condition was vector-subtracted from that of the other condition, the resulting vector squared per bin, and summed across all bins. For comparisons between more than two conditions, the sum of squared differences was calculated for each pair of conditions, then summed across all pairs. This test statistic was used for testing any significant differences in mPFC neuronal firing patterns 1) between opposite running directions on each track arm in which case running laps were permutated between inbound and outbound directions, 2) between (when centered on) replay and non-replay events in which case each hippocampal population firing event was randomly reassigned as replay or non-replay, and 3) between (when centered on) single-arm replays representing different track arms in which case each single-arm replay was randomly reassigned as representing a track arm. For testing a significant effect of the interaction between

running direction and position on a track arm, on the firing pattern of each mPFC neuron during active running, the test statistic *F* of a two-way ANOVA on position and direction was used as the test statistic of the permutation test, in which firing rates from all position bins, all laps, were shuffled across positions and directions. Note that in all permutations the trial number in each condition was kept the same as that of the original data.

4.2 Results

We conducted multi-tetrode recordings simultaneously in the dorsal CA1 area and the medial prefrontal cortex (specifically targeted the prelimbic cortex, tetrode depth 2mm-3.5mm from brain surface) in four rats. Recordings started since the first time rats were exposed to the asymmetric Y-shaped maze. Rats freely explored the maze and were rewarded chocolate milk at arm ends according to an alternation rule. One recording session was selected from each rat for data analysis (Rat 1 Day 4, R2D2, R3D1, R4D1), in which we obtained reasonable numbers of single units from both brain areas and of running laps on all arms. During these sessions, novelty of both the environment and task likely remained, which might have involved active processes in the hippocampus and mPFC for spatial learning and rule acquisition. For CA1, putative pyramidal cells with peak in-field firing rates higher than 1 Hz were used to detect replay. In mPFC, putative pyramidal cells, defined as single units whose mean peak-to-trough spike widths were wider than 0.35 ms, except for noisy and ultra-low firing-rate pyramidal units, entered data analysis; interneurons were excluded from analysis.

4.2.1 CA1 replays representing different paths were detected in abundant numbers

We estimated position representation by the ensemble of recorded place cells using a Bayesian decoding method introduced by (Davidson *et al.*, 2009). During stopping periods at arm ends, we identified replay events as epochs with high population firing rates during which the posterior probabilities showed high correlations between position and time; we also required that the trajectories represented by high-probability pixels span sufficient durations and distances. Note that overlapping time bins (20ms bins moving in 10ms steps) were used in this study to increase the accuracy of position estimation and replay identification. Using the 66, 96, 88, and 58 cells recorded from rats 1-4, we identified large numbers of replay events from each rat, with a procedure specifically designed to identify single-arm replays which represented individual arms (R1D4: N = 402, R2D2: N = 799, R3D1: N = 781, R4D1: N = 397; see examples in Figures 4.1C,H,F) and joint replays which extended across pairs of arms (R1D4: N = 32, R2D2: N = 164, R3D1: N = 195, R4D1: N = 106; Figures 4.1D,E,G). All six paths, namely single C, R, L arms, and joint C ↔ R, C ↔ L and R ↔ L trajectories, were found to be represented by replay in each rat.

4.2.2 Running direction modulated mPFC neuronal activities

(Jung *et al.*, 1998) demonstrated evidence of running-direction correlates of PFC activities in rats performing an eight-arm radial maze, spatial working memory task. They found that a small fraction of PFC neurons showed firing-rate differences between inward and outward running directions when crossing the middle of maze arms, and that a larger

percentage of the neurons showed direction-selective increases or decreases in firing rate during either inward or outward running behavior. To analyze this property of PFC activities during active maze running, we plotted firing rates of individual neurons against position for each lap of running, on the three track arms and in the inbound and outbound directions separately (Figure 4.2A). Consistent with previous findings, we found that in our experiments mPFC neurons showed highly consistent firing patterns over position across laps with the same running direction which were however considerably different between opposite running directions on the same arm. For example, Figure 4.2B shows an mPFC neuron exhibiting gradually increasing firing rate as the rat ran from reward area (left) to choice point (right) on C arm (Top panel: upper section and blue curve). The same neuron showed a nonlinear firing pattern against position as the rat ran back to the C arm reward area from choice point (Top panel: middle section and red curve), with relatively lower firing rates close to the choice point and relatively higher firing rates close to the reward area, directly contrasting its firing pattern in the opposite, departure direction. Such apparent firing pattern difference persisted on all individual arms for this neuron (see its firing activities on R and L arms in Figure 4.2B, middle and bottom panels), and for another example neuron from the same recording session (Figure 4.2C), while the rat's running speed pattern over position did not show such degree of contrast between opposite directions on any arm (Figure 4.2D), which could not have accounted for the differences observed in neuronal firing-rate patterns. Two tests were used to measure significant difference, both utilizing permutations which do not require assumptions of independence of firing rates in successive position (or time) bins or normality (Steinmetz *et al.*, 2000). The test statistic

of the first method is squared differences of mean firing rates, per position bin, between the opposite running directions summed across all bins; the second method used the test statistic F of a two-way ANOVA with position and direction being the two factors and accordingly permuted both position bins and running directions. Among 54 mPFC pyramidal neurons recorded from all rats, 80% and 65% in the two statistical tests respectively, showed significant differences ($p < 0.05$) in their firing patterns between opposite running directions on at least one arm, while around 20% showed significant differences on all three arms in either test (Figures 4.2E,F). Thus, during active running behavior on the Y maze, a majority of mPFC neurons' firing activities were modulated by either running direction alone, or an interaction between position and direction.

4.2.3 Reward conditions affected mPFC activities

The prefrontal cortex is densely innervated by the midbrain dopaminergic systems, and is suggested to play a role in establishing associations between task rules or cues and the desired actions or subsequent reward (Miller & Cohen, 2001). To examine the possible effects of reward conditions on mPFC neuronal activities in our task, for each arm we separated visits to the reward area at arm end into rewarded and unrewarded trials (note that visits to the C–arm reward area were always rewarded). The spike train from each neuron during each trial was aligned either to the beginning of reward consumption, as judged by visual inspection of overhead camera recordings, for rewarded trials; or to the time point of crossing reward area edge determined based on position recordings, for unrewarded trials. Systematic quantifications were not performed due to the difficulties and inaccuracies in determining the start of reward consumption based on overhead camera recordings (a more effective method would be using laser beams to detect tongue

intrusions into food wells). Nonetheless, the current method still revealed evidence of reward-related effects on mPFC single neuron activities. For example, Figures 4.3A-D show a neuron with abruptly increased firing rates during reward consumption which extended for long time courses (~10 sec); entering reward areas during unrewarded visits, on the other hand, did not alter its prior, very low firing activities. Moreover, this neuron fired at a higher rate when reward was received at the L–arm end as compared to when reward was received at the C– or R–arm end which elicited similar firing activities. A different neuron exhibited elevated activities in both rewarded and unrewarded conditions, while firing rates were the highest during unrewarded visits to the R–arm end (Figures 4.3E-H). These observations suggest that mPFC neuronal activities were affected not only by the receipt or omission of reward, but also by the spatial location at which these outcomes were revealed to the animal. This spatial dependence may reflect the differences in reward values attached to the three arms that were inherent to our task design: visits to the C–arm end were always rewarded whereas visits to the R– and L–arm ends were alternately rewarded; meanwhile reaching the L–arm end required the most effort due to the longer length of this arm.

4.2.4 Change of medial prefrontal activities upon replay occurrence

To address the main question of whether evidence of interaction between hippocampal replay and prefrontal activities exists, for each mPFC neuron we extracted and aligned its spikes fired around occurrences of replay to look for consistent changes in firing activities. These epochs of spikes can potentially be aligned by the beginning, center, or end time points of replay events – without any a priori hypothesis we simply chose to use the center of replay for alignment. Figure 4.4 shows example mPFC neurons which

exhibited apparent changes in firing rate, either increasing or decreasing, consistently at the moments of replay occurrence, with the largest departures from baseline firing rate occurring very close to the centers of replay events (0 ms in panels A-D). Note that all identified replays from each rat are included in this analysis regardless of the specific trajectories they represented. As a control, such alignment method was applied to high spike density events (replay candidate events) which were determined not to contain any replay structure (Figures 4.4A-D, black curves). This comparison showed that although neuronal firing rates also changed in the same directions around non-replay events, the changes were much less prominent than those observed around replay events. In fact, 41% (22/54) of mPFC neurons showed significantly different firing-rate changes from baseline activities upon the occurrences of replays than upon the occurrences of non-replay events ($p < 0.05$, permutation test on sum of squared differences; Figure 4.4E). Therefore, our data showed strong evidence that hippocampal replays and prefrontal neuronal responses are tightly coupled brain activities instead of independent processes.

4.2.5 Replay – mPFC coactivity depended on replay content

We hypothesized that replay and prefrontal activities interact in an information-dependent manner which may serve as an essential mechanism supporting important functions of the hippocampal-prefrontal network. The next important question is thus whether this interaction communicates any relevant information content, such as trajectories along the Y maze which we showed were accurately represented by replay in Chapter 3. Since the majority of replay events represented individual arms, we compared each mPFC neuron's firing activities centered on single-arm replays representing different arms (Figure 4.5). Interestingly, such separation by replay representation

revealed drastically different firing patterns in numerous mPFC neurons. Moreover, the specific differences were often different from neuron to neuron. For example, one neuron (Figure 4.5A) showed firing-rate increases by an average of almost 8 Hz when replays representing either the right or left arm occurred while showing minimal changes at occurrences of replay representing the central arm; a different neuron (Figure 4.5B) showed decreases in firing rate to C- and L-arm replays, but increases to R-arm replays; a third neuron (Figure 4.5C) showed increases in firing rates to all single-arm replays although the amount of increase was different between replays representing different arms; another neuron (Figure 4.5D) showed similar firing-rate increases around replay onsets but different 'after effects' toward or after the end of replays. Across mPFC neurons of all rats, 24% (13/54) showed significantly different firing patterns between replay events representing different arms of the Y maze ($p < 0.05$, permutation test on sum of squared differences). Thus, the temporal correlation between mPFC neuronal activity changes and replay events was indeed modulated by, in our experiments, the trajectory information contained in replay. This information-content dependence suggests active processing and communication of spatial trajectory information in the functional hippocampal-prefrontal circuit.

To further investigate the diversity in neuronal firing patterns contingent on replay representation, we visually classified each neuron's responses as excitatory (Ext), no change (N/C), or inhibitory (Ihb), at the occurrences of the C–, R–, and L–arm replays separately. These classifications were demonstrated as highlighted nodes onto a three-dimensional grid of response types against replay arm representations such that each

individual neuron's firing pattern was matched to a particular node (Figure 4.5E). The 13 mPFC neurons which showed significant differences in their firing patterns centered on replays depicting different arms largely occupied separate nodes, with only three pairs of cells showing the same classification results within the pair. Thus, instead of showing a unified pattern of modulation by replay content, these neurons exhibited rather diversified activities with each neuron responding to different trajectory representations in a distinct manner.

Examining mPFC neuronal activities at the occurrences of joint replays was challenging, due to the much smaller numbers of joint-replay events identified. To look for consistency in mPFC responses between joint replays and single-arm replays, we oriented and aligned joint replays of each trajectory (*e.g.* joint replays of CR) such that the represented trajectory in each event was of the same orientation (*e.g.* C → R) with the representation of one arm end (*e.g.* C–arm end) temporally aligned across all replay events; such procedure was repeated for the opposite orientation and arm-end alignment (*e.g.* R → C trajectory orientation with all events aligned to the R–arm end; see Figures 4.6A,D,G). The spike train of each mPFC neuron was reshaped in the same way, with each brief epoch of spikes occurred around a joint-replay event oriented and aligned in the same way as the time frame, *i.e.* trajectory-specific subregion, of that joint-replay event (Figures 4.6B,E,H). The firing pattern of one particular neuron as revealed by this analysis showed remarkable consistency in its responses to the spatial representation of replay events. This neuron exhibited an increase in firing rate precisely aligned to the brief moment when the R–arm end was represented by joint replays of CR, while firing-

rate changes at the representation of the C–arm end was minimal (Figures 4.6B,C). This neuron also exhibited an increase in firing rate aligned to the representation of the L–arm end during joint replays of CL, while showing little activity changes at the representation of the C–arm end (Figures 4.6E,F). During joint replays of RL, however, this neuron did not appear to differentiate between the R–arm and L–arm ends, showing an increase in firing rate in between the representations of the two arm ends (Figures 4.6H,I). Interestingly, this same neuron showed a considerable increase in its firing rate only at the occurrences of the single R– and L–arm replays (Figure 4.5A), matching its activity pattern with regard to the spatial representation of joint replays, *i.e.* large increases in firing rate specific to the representations of the R– and L–arm ends. Therefore, evidence exists that mPFC activities were indeed tuned to the spatial information content signaled by hippocampal replay events in a consistent manner.

4.3 Discussion

4.3.1 Medial prefrontal activities were modulated by important task components

We analyzed mPFC single unit activities during active track running as well as how they were affected by behavioral outcomes at arm ends. A robust observation was that the majority of mPFC neurons were modulated by running direction alone or an interaction between position and direction, on some or all of the arms. Some neurons exhibited very similar firing patterns in the same running direction on all three track arms, in both the inbound and outbound directions (*e.g.* Figures 4.2B,C). We suggest that these neurons may not represent the animal's head direction as neurons in *e.g.* the subiculum and

thalamus were found to represent, but rather reflect cognitive processes that may have taken place when the animal was approaching the choice point facing two potential paths, or approaching a reward area after a path was already chosen, such as decision making and reward expectation. Furthermore, we found that mPFC activities were affected by reward outcomes in an arm-identity dependent manner, which we suggested reflected the motivational salience attached to the arm ends as imposed by our task design and not spatial location per se. Following this interpretation, we would expect to observe, for example, if reward contingencies on the short C– and R–arms were to be switched such that visits to the arm located on the right-hand side are now always rewarded whereas visits to the centrally-located arm are now alternatively rewarded with visits to the long, L–arm, that reward-outcome modulated neuronal responses would also switch patterns between the short arms following the new reward contingencies, instead of remaining the same following the fixed spatial locations of the arms. Nonetheless, we found strong modulations of mPFC neuronal activities by important aspects of the Y-maze task, suggesting their active involvement in the brain processes required for task performance.

4.3.2 The possible role of mPFC – hippocampal replay interaction in decision making

Hippocampal activities have been shown to correlate with neuronal processes in brain areas other than the prefrontal cortex at fine time scales. For example, (Ji & Wilson, 2007) found coincident primary visual cortical and hippocampal replay sequences in SWS which reflected the same awake experience (the visual aspect of the experience was likely orderly encountered local visual cues that were encoded by a subset of visual cortical cells with spatially bounded firing fields), presumably contributing to long-term

storage of visual memory in the primary visual cortex. (Lansink *et al.*, 2009) presented evidence for correlated firings of hippocampal-ventral striatal cell pairs while rats were running for reward, and for the recurrence of such pairwise correlations during postbehavioral sleep which may serve to consolidate place-reward associations. Similarly, the functional consequences of mPFC firing-rate modulation upon hippocampal replay occurrences may well lie in the specialized functions of the mPFC, notably decision making. In fact, the process of decision making could be decomposed into four steps, with the second step being evaluating 'action candidates (or options) in terms of how much reward or punishment each potential choice would bring' (Doya, 2008), and the prefrontal cortex has been implicated to be the brain area that performs this task – it holds and manipulates in working memory task-relevant information received from other brain areas and computes the option that potentially leads to the best outcome (Floresco *et al.*, 1999; Kable & Glimcher, 2009). In a spatial navigation task like ours the animal is continuously obliged to choose a path leading to reward, trajectory information is crucial for decision making. Hippocampal replay events are well suited to convey this information, as have been shown by many to 1) faithfully represent possible trajectories in extended environments, and 2) involve synchronized network-wide spiking activities powerful enough to exert large postsynaptic impacts on downstream neurons hence transmitting coherent pieces of information cross-structurally. Indeed, mPFC neurons responded strongly to hippocampal replay in our study; importantly, individual neurons in a subpopulation differentiated the information content represented by replay exhibiting significantly different firing patterns coincident with replays depicting different track arms, each in a distinct manner. We propose the intriguing possibility that

the heterogeneous responses among mPFC neurons may constitute decision making processes utilizing trajectory information communicated by hippocampal replay, such as evaluation and comparison of potential paths. The collective mPFC representation coincident with replay may be revealed with the capability of obtaining larger numbers of recorded mPFC neurons per recording session, in resemblance to decoding the focused spatial representation of a place cell population knowing the heterogeneous responses of individual place cells to each spatial location. Such investigation is likely to require a better understanding of mPFC neuronal representations during task performance as well.

4.3.3 Network mechanisms involved in the interaction between prefrontal activities and hippocampal replay

We characterized hippocampal replay and its relationship with mPFC activities during intermittent awake immobile periods within the navigational environment. In contrast, most previous studies relevant to ours focused on post-task SWS episodes, and have now depicted a plausible picture of the interplay between the hippocampus and the neocortex during SWS: prominent sleep spindle and delta oscillations in the neocortex may trigger the initiation of hippocampal SWR epochs, by *e.g.* modulating membrane potential of hippocampal interneurons (Hahn *et al.*, 2006) thus influencing hippocampal intrinsic rhythms, or driving selective 'burst initiators' residing in the CA3 by the specific neocortical cell assemblies active during the spindles (Csicsvari *et al.*, 2000; Sirota *et al.*, 2003). Importantly, this activation process may only target unique groups of hippocampal neurons, and their represented information, for replay during the ensuing SWR event, which is then sent back to various neocortices to orchestrate replays of different modalities in these areas, involving the still active neocortical cells that originally

initiated this two-way process (Marr, 1971; Sirota *et al.*, 2003; Isomura *et al.*, 2006; Ji & Wilson, 2007). This well documented sleep mechanism provides several insights for interpretation of hippocampal-prefrontal interaction in the awake immobile state: first, replay might not be spontaneously generated by the hippocampus, but instead specifically triggered by mPFC to retrieve selected trajectory information for the ongoing decision making process (which could possibly take place during stopping periods at reward areas, besides the moments when approaching the choice point); secondly, awake hippocampal replay might also evoke replay activities in functionally connected regions, including particularly, coordinated reactivation of reward information which is also crucial for decision making. Hence, the interaction between prefrontal activities and hippocampal replay sequences may share common network mechanisms in different behavioral and brain states, yet acting as the fundamental mechanisms in different global brain functions serving the ongoing behavioral needs, namely decision making processes during the awake, task performance state, and memory consolidation during the offline, SWS state.

Figure 4.1

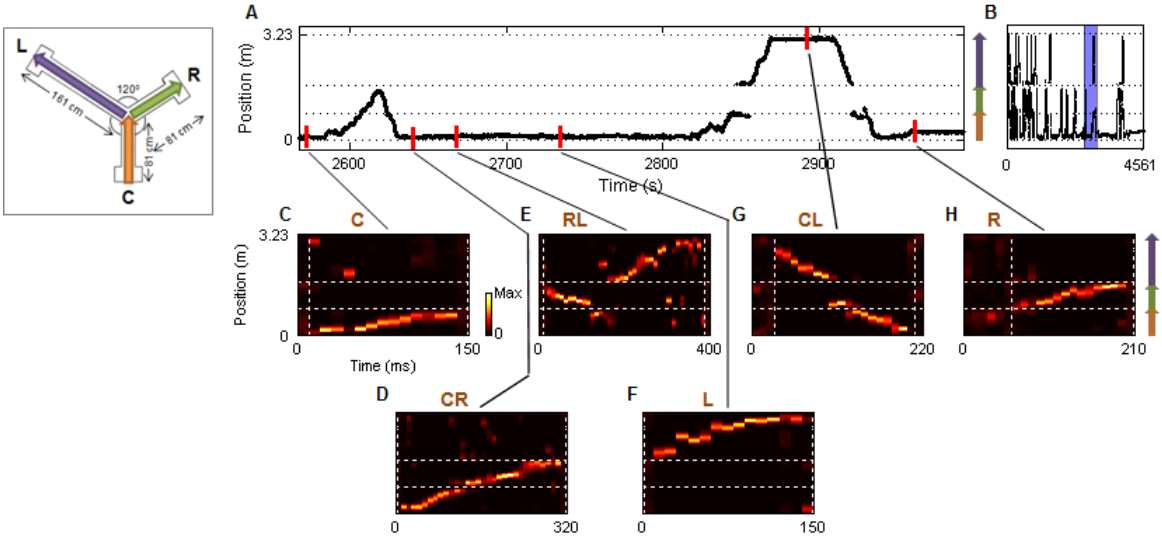

Figure 4.1 Replays representing single and joint arms of the Y maze

(A) Linearized position of Rat 3. Horizontal dashed lines indicate arm boundaries. Colored arrows on right indicate arm alignment along linear axis, which correspond to the arm labeling in inset on left: C: central arm, R: right arm, L: left arm.

(B) Recorded position of Rat 3 in the entire first recording session (~ 76 min). Shaded blue area indicates the period shown in (A).

(C-F) One example replay event of each path. To demonstrate replay quality in our data, positions were decoded in 10-ms non-overlapping bins in this figure. Letters above the panels indicate the single- or joint-arm represented by each example event.

Figure 4.2

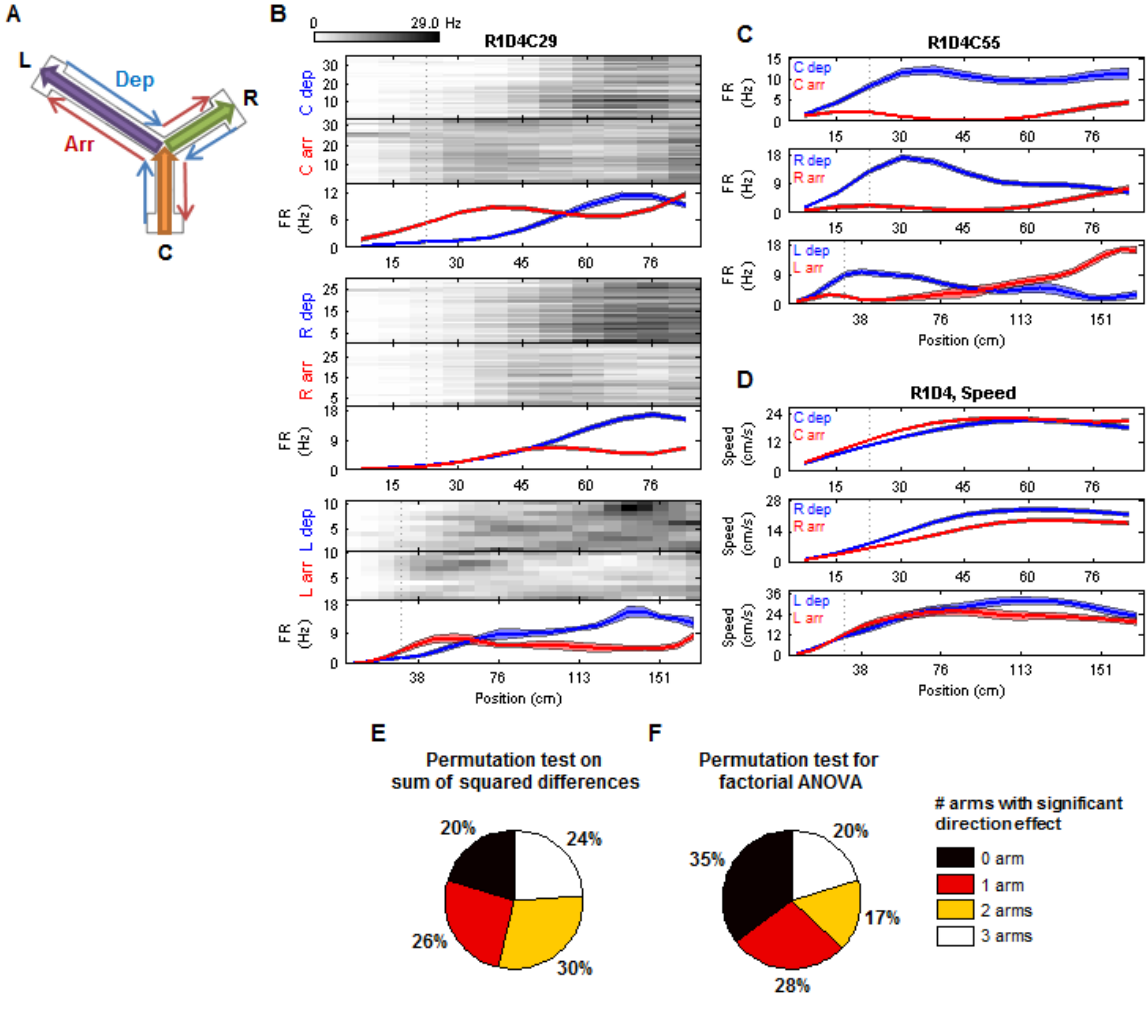

Figure 4.2 mPFC neuronal firing activities were modulated by running direction

(A) Running towards reward areas is arrival (Arr, red arrows); running towards choice point is departure (Dep, blue arrows).

(B) A single mPFC cell's firing rate in each position bin during each lap of running on each arm (each row) is color coded in grey scale. Reward areas were always oriented to the left side, with vertical dotted lines marking the position bins in which the inner edges

of reward areas located, while the choice point was always oriented to the right. Arrival laps were separated from departure laps (see color notations on left). Top to bottom: running on C arm, R arm, L arm. Red curves: mean ± SD of firing rates across all arrival laps on each arm; blue curves: mean ± SD of firing rates across all departure laps on each arm.

(C) Mean firing patterns per running direction, per arm, of a different mPFC neuron recorded from the same rat, same recording session.

(D) Mean running speed patterns per running direction, per arm, of the same rat, same recording session.

(E,F) Percentages of mPFC neurons exhibiting significant direction modulation during running on 0, 1, 2, or all three arms, quantified in two permutation methods.

Figure 4.3

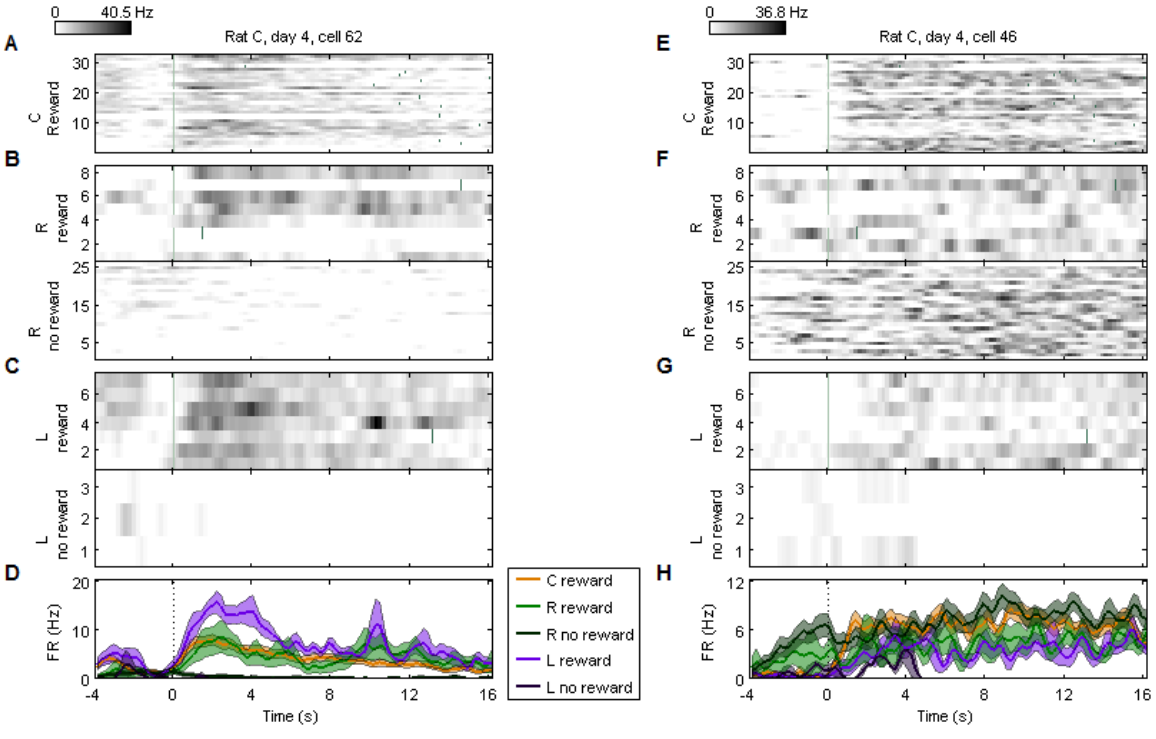

Figure 4.3 mPFC neuronal activities were likely affected by reward conditions

(A) A single mPFC cell's firing rate in each 200ms time bin during each visit (each row) to the C–arm reward area (always rewarded) is plotted in grey scale and aligned to the beginning of reward consumption (0 s, indicated by vertical line) estimated from the overhead camera video recording. Estimated consumption finishing times, if ≤ 16 s, are indicated with ticks.

(B,C) The same cell's firing rates during visits to the R– and L–arm reward areas, with rewarded and unrewarded trials separated. For unrewarded visits, 0 s corresponds to the time when the rat crossed a position threshold marking the edge of the reward area.

(D) Mean firing rates averaged across trials for the different reward sites and outcomes (see legend on right).

(E-H) Reward-site firing activities of a different mPFC neuron recorded in the same recording session are plotted in the same manner.

Figure 4.4

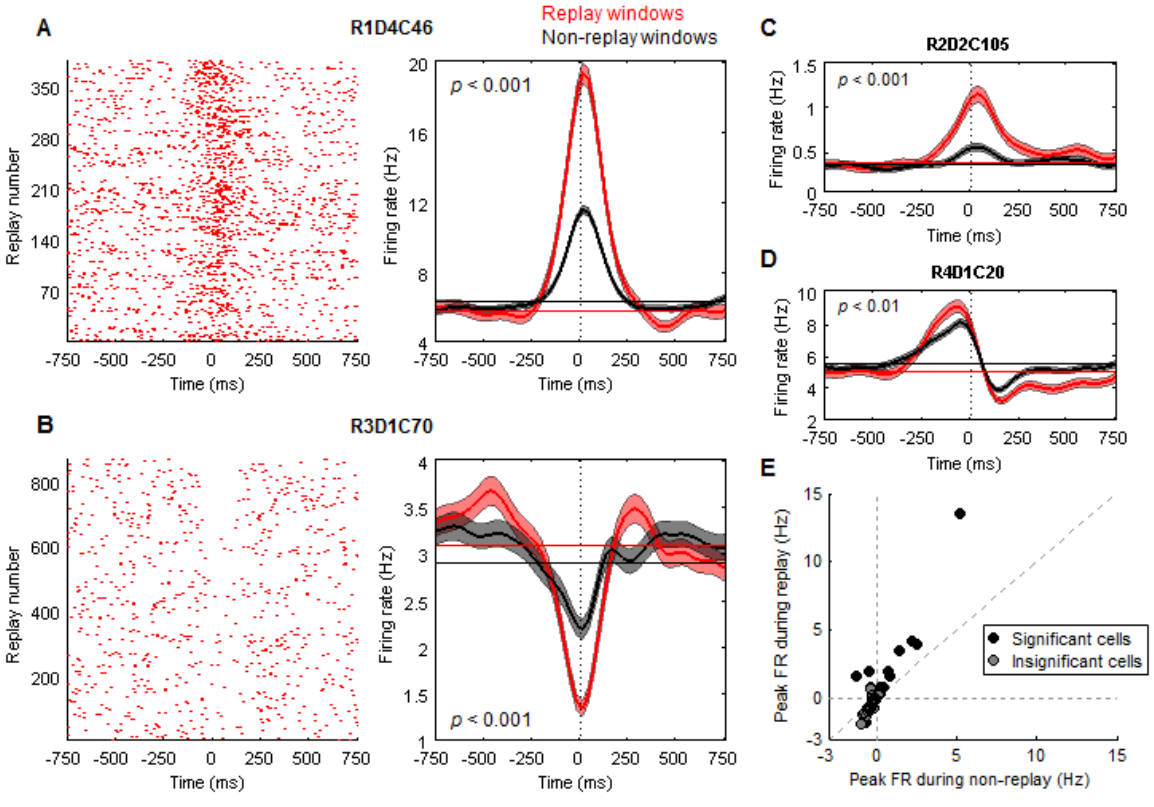

Figure 4.4 Medial prefrontal neurons exhibited larger activity changes at occurrences of replay than at occurrences of non-replay event

(A-D) Panels A,B left: raster plots of example mPFC cell firing activities aligned to the centers (0 ms) of identified hippocampal replay events (all single- and joint-arm replays included). (A,B) right & (C,D): mean ± SD of each cell's firing activities across all replay events (red), and all non-replay events (black). Also shown for each neuron are mean baseline firing rates separately calculated for replay events and non-replay events, using firing rates in the adjacent, -2 sec to -1 sec and 1 sec to 2 sec periods.

(E) The largest deviation from baseline firing rate within ± 0.6 secs, in each neuron's mean firing activities centered on replay events, was plotted against that obtained from non-replay events. Neurons showing significant differences in baseline-subtracted firing activities between replay and non-replay events are shown in black; the rest of the neurons in grey.

Figure 4.5

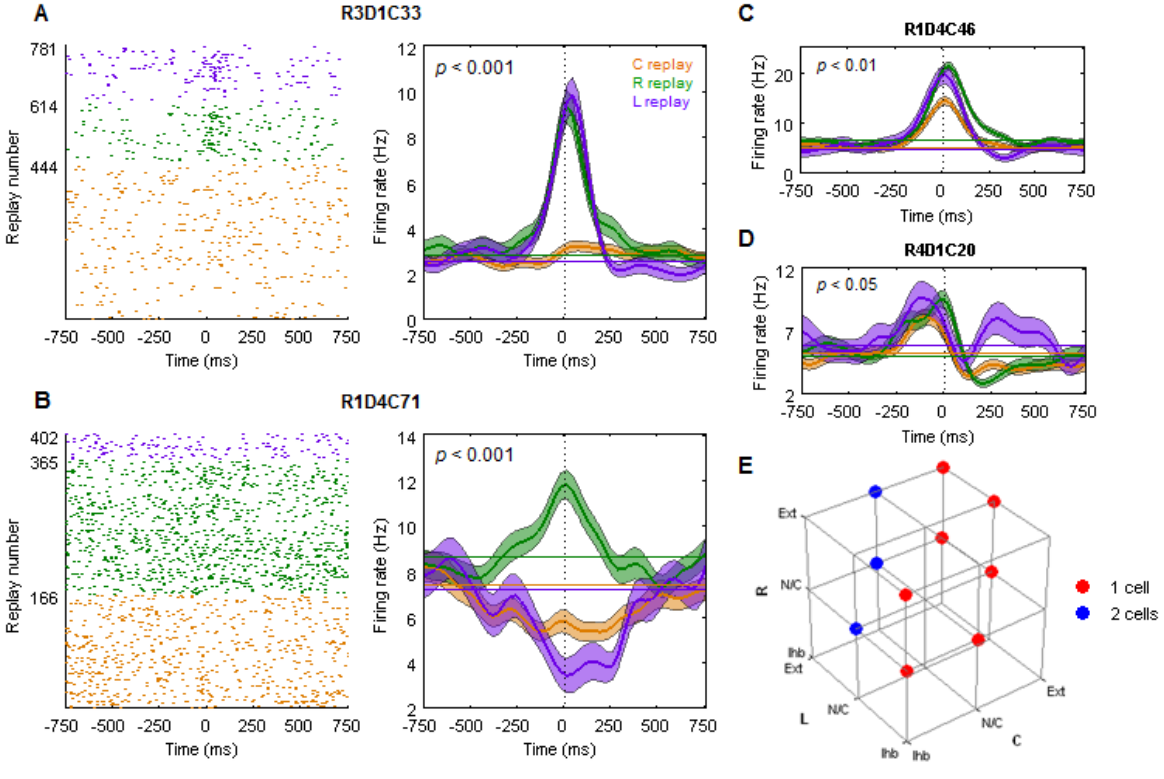

Figure 4.5 Medial prefrontal neurons exhibited different activity patterns at occurrences of replays representing different arms

(A-D) Format similar to Figures 4.4A-D. (A,B) Left panels: raster plots of example mPFC cell firing activities aligned to the centers (0 ms) of single-arm replays. Spikes occurred around single-arm replays representing each arm are labeled with a different color (see legend in (A)). (A,B) Right panels & (C,D): mean ± SD of each cell's firing activities across all single-arm replays representing each arm is plotted in the corresponding color.

(E) Thirteen cells which showed significance are placed on nodes indicating whether their firing rates increased (Ext), did not change (N/C), or decreased (Ihb) at the occurrences of single-arm replays representing the C, R, L arm.

Figure 4.6

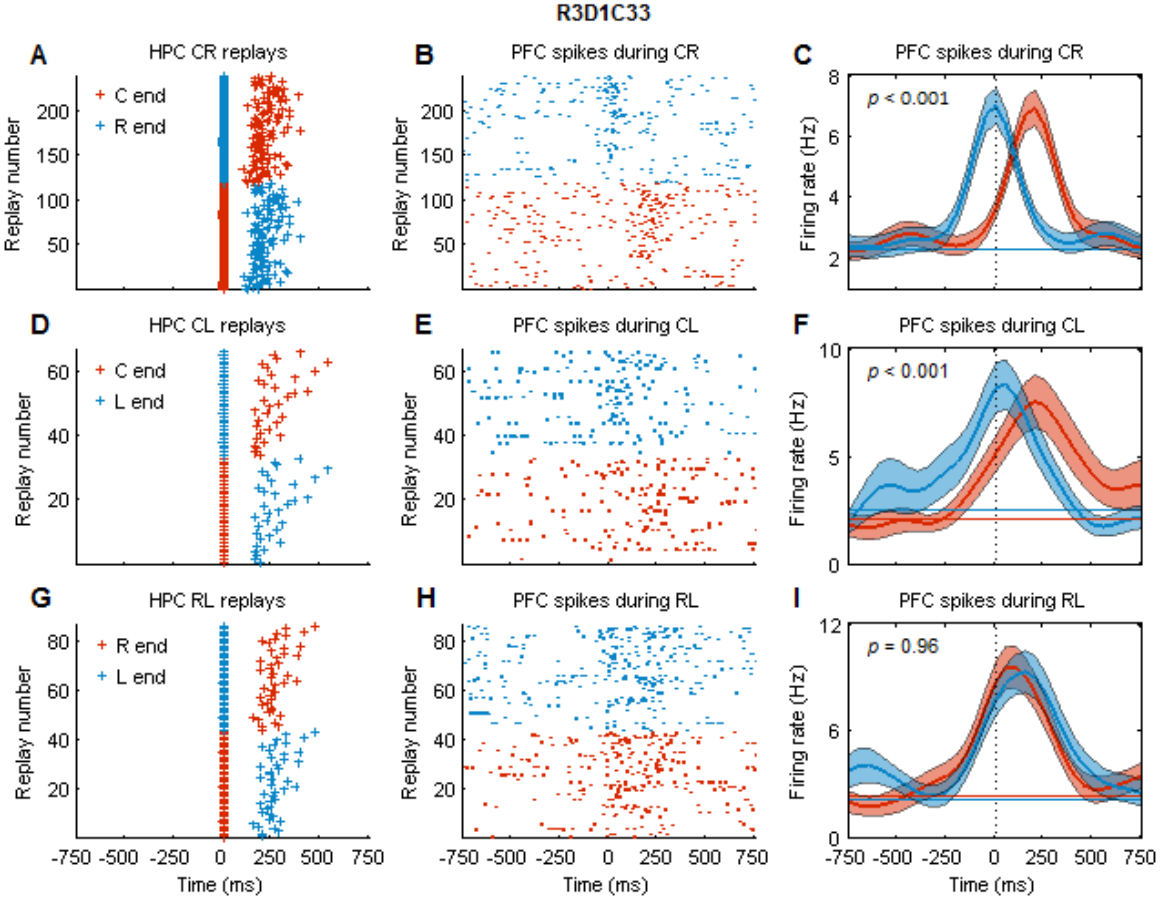

Figure 4.6 An example mPFC neuron's firing patterns during joint replays

(A) Joint CR replays from rat 3, session 1 were reoriented and realigned such that representations of the C–arm end are at 0 ms while representations of the R–arm end land at positive times (panel lower half), or the opposite (upper half).

(B) A single mPFC cell's spikes occurred around CR replays were aligned in the same way as in (A) with row-to-row correspondence.

(C) Mean ± SD of the same cell's firing activities with either alignment is plotted in the corresponding color.

(D-F) The same mPFC cell's firing activities occurred around joint CL replays were aligned to the replay representation of the C–arm end or L–arm end.

(G-I) The same mPFC cell's firing activities occurred around joint RL replays were aligned to the replay representation of the R–arm end or L–arm end.

Chapter 5 General discussion

The hippocampal place cell system exhibits highly coherent representations during active running as well as intermittent SWR epochs in quiet wakefulness and sleep states, whereby firing activities across the neuronal population collectively represent a specific spatial location at each moment in time. The ability to truthfully decipher such representations was crucial to our studies, which has been greatly aided by the Bayesian decoding method introduced by (Davidson *et al.*, 2009) that holds major advantages over previous analysis methods. The Bayesian method utilizes the entire place tuning curve of each neuron in estimating position representations, as opposed to only the peak firing locations that correlation methods use to relate run-time representations to SWR-associated spike patterns, which often results in excessive information reduction as place cells tend to fire at different locations in many environments. A related advantage is thus that the Bayesian method is not restricted to the shape of the environment, and is theoretically applicable to any nonlinear, complex environment that the experimental design might require. Thirdly, the Bayesian method captures the form of representation of the place cell system, that the contribution of spikes or silence from each neuron is counterbalanced by the activities of all the other neurons in achieving a collective representation across the population; it also takes into account neuronal firing rates such that spikes from low firing-rate neurons carry less weight in the position estimates. Consequently, the Bayesian method is very robust to a reasonable level of the inclusion of electric noise or incorrectly-assigned spikes often present due to spike-sorting errors,

and is beneficial for studies which do not focus on the spatial responses of individual neurons.

It is important to note that our replay identification method, which was based on position estimates from the Bayesian decoding analysis, was specifically designed to detect single- and joint-arm replays which progressed with the same momentum in position either between an arm end and the choice point or between two different arm ends. This method is therefore not sensitive to other possible forms of trajectory representation such as one that travels back and forth on the same path which has been observed in our data, although single- and joint-arm replays did appear to be dominant upon visual inspections. Moreover, the possibility exists that replay events could simultaneously represent different paths within the same environment, which if true, would require new explanations about the organization of replay structure and the mechanism of replay generation. In our replay identification method, we segmented each high spike-density candidate event into six 'trajectory-specific subregions' and determined for each subregion whether the structure of decoded positions represented a coherent trajectory. Across all rats, 1452 events had at least one subregion with identified replay structure, among which 1188 (81.8%) events had exactly one subregion with identified replay structure. Among the rest of the events, in which the hypothesized condition of different arms being replayed at the same time could have occurred, the majority (252 events, 17.4%) contained one joint replay with one or both of its component single-arm sequences also passing criteria, *e.g.* a CR joint replay whose C, or R, or both C and R segments also identified as replays on their own. For these joint-replay events, we found

that the temporal overlap between the two component single-arm segments only occupied, on average, 4.1 ± 0.3% of the entire joint-replay durations. Thus, there was very little overlap in time between the representations of different arms during joint replays. The remaining 12 (0.8%) events are displayed in Figure 5.1. It can be seen that many of these events contained two non-overlapping single-arm replays which seemed to form coherent joint sequences which however did not pass our criteria. Therefore, we did not see evidence in our data that different arms were replayed at the same time in a significant number of events.

We analyzed the properties of hippocampal replay sequences that occurred during the animals' very first exposure to a novel environment. Although the place responses of individual place cells were not the focus of our study, they do determine position estimates and hence the likely changes in place responses with experience will directly affect the representation of replay events. A few previous studies have attempted to determine the speed of development of place fields in novel environments, which have reported not-entirely consistent results. It has been shown that many place cells began to fire within their steady-state place fields upon the animal's very first entry into the place field locations (Hill, 1978), while (Wilson & McNaughton, 1993) indicated that the stabilization of place fields took about 10 min of experience in the novel environment. A more recent and more sophisticated analysis showed that although most CA1 cells were active during the first passage of a novel arm, place fields exhibited rapid changes during the initial moments of exposure and required at least 5-6 min of experience to stabilize (Frank *et al.*, 2004). It should be noted that it is generally difficult to estimate the time

course of development of place fields since place field calculation requires the accumulation of spike and position data. In our analyses, place fields calculated from whole-session data, *i.e.* steady-state place fields, were used to decode replay. Consequently, if at the very beginning of exposure certain place cells were silent, or fired at a different location or rate (Frank *et al.*, 2004), replays occurring at that time would not have been reliably detected using the steady-state place fields. Hence, our estimate of how rapidly after experience replay occurs should be considered conservative, since replay could in fact have occurred earlier. Nonetheless, even with this analysis method, replay can be detected in significant numbers after very little experience in a novel environment. Our other results should not have been affected by the initial changes in place fields, as the majority of replay events occurred at later times in the recording sessions when place responses had already stabilized (recording session durations were between 76 min and 130 min).

A related question is whether replay properties changed across days as the spatial environment as well as the reward rule became learned. Such changes may be contributed to by place-field changes between recording sessions, or/and changes in the organizing structure of sequential replay itself. We have not repeated our analyses for the subsequent recording days, mainly due to the fact that either animal behavior or cell yield was not consistent across days. Questions such as how the ratio between single-arm and joint replay event numbers, the proportion of directional replay, and the composition of reverse versus forward progress through learning are certainly very interesting, but will require the collection of data with more consistent quality across many consecutive days.

Based on our current findings, we propose that hippocampal replay occurs rapidly and that replay representation accurately reflects environmental topology. A modified experimental design, which separates the animal's experience of the novel environment into restricted segments, may be used to provide more direct evidence for these statements: without any previous exposure to the Y maze, the animal is placed at the baited C-arm end just as in the original experimental design. However, the animal is immediately taken out of the Y maze as soon as he reaches the choice point for the first time, ideally after only one unidirectional traversal on the C arm, and is placed in the sleep box isolated from the Y maze for a certain period of quite wakefulness/sleep state recordings, which will be used to test for significant replay representation of the C arm, providing evidence for rapid one-trial spatial learning (Figure 5.2A). The animal is then returned to the C-arm end, is expected to wander into a new arm, *e.g.* the R arm, and is immediately taken out of the Y maze once the R-arm end is reached. Replays representing the single C and R arms as well as the joint CR trajectory are expected to occur during the second sleep-box recording (Figure 5.2B). Placed back at the C-arm end again, the animal travels to the third arm, *e.g.* the L arm, either voluntarily or guided by the experimenter or a small barrier at the choice point blocking off the R arm, and is immediately taken out of the Y-maze upon reaching the L-arm end. During the following sleep-box resting period, replays representing all single- and joint-arm paths are expected to be observed (Figure 5.2C), especially the ones that represent the never-experienced joint-arm trajectory (*e.g.* R ↔ L); at the meantime, the common segments of each pair of joint replays are expected to be represented by the same population of neurons with the

same firing rates, as observed in the current experimental design (Figure 3.3). Findings of such nature will provide strong evidence for a rapidly formed hippocampal representation of the overall spatial structure of a novel, complex environment, as well as the emergence of structurally-correct novel routes reflected in the trajectory representation of replay events. Subsequently, the animal will be returned to the Y maze for a long period of recording following the original experimental procedure, to collect abundant spike and position data during active running for place-field calculations. Place tuning curves may also be computed using the initial single-lap experiences with the application of a much wider Gaussian window for sufficient smoothing.

Our examinations of hippocampal replay have mainly focused on its spatial representation, yet replay has also been shown to possess behavioral correlates. For example, (Pfeiffer & Foster, 2013) demonstrated that SWR-associated place-cell sequences occurring immediately prior to movement in a spatial memory task depict the future trajectory that the animal will take to the remembered goal location. Moreover, prefrontal neuronal activities coincident with replay may not only differentiate between different trajectory representations (Figure 4.5), but also the same spatial representation in different behavioral conditions, *e.g.* single-arm R replays occurred at the R-arm end during rewarded versus unrewarded visits. We have attempted to separate replays representing the same path based on 1) the arm ends at which they occurred, 2) rewarded versus unrewarded stopping periods, 3) matching to the immediate past or the immediate future trajectory taken by the animal, 4) matching to the immediate past trajectory leading to reward during rewarded visits or any other trajectory occurred during the same

stopping periods, but found that we did not have sufficient data to further subdivide our replay events into location, decision, or outcome based categories. It should be noted that (Pfeiffer & Foster, 2013) did report heterogeneity in the expression of replay sequences with some sequences not going to the goal. We expect that such heterogeneity does mask choice-related biases in a task with only two future paths (Gupta *et al.*, 2010).

We also attempted to correlate prefrontal neuronal response patterns coincident with replay occurrences to those we quantified during task performance, with the hypothesis that, for example, a prefrontal neuron that only fired during running on the C arm may exhibit higher firing rates upon occurrences of the single-arm C replays as compared to single-arm R and L replays. While evidence for this type of correlation was not found in our data, it is possible that the low numbers of medial prefrontal neurons we were able to record prevented us from making such observations. Efforts to increase cell yield in the prefrontal cortex are also necessary for the purpose of revealing representations at the population level – although much heterogeneity was found in all aspects of prefrontal responses we analyzed, unified representations such as coherent decision making processes (*e.g.* the evaluation of a specific path) may arise across the total population or each subpopulation. Achieving large recorded cell numbers is difficult, as cortical neurons are very scattered. One possible way to improve recording is to implant the drive at a small angle of 5^{o} instead of vertically, such that tetrodes will travel diagonally to reach the deep IV and V layers parallel to the sagittal sinus where the cell bodies of medial prefrontal neurons are located (Jung *et al.*, 1998).

Finally, the spatial aspect of hippocampal functions has also been shown in humans based on patient studies. For example, among hippocampally lesioned human patients getting lost and forgetting where objects have been placed are among the most common symptoms accompanying memory loss (Bird & Burgess, 2008). Schizophrenic patients also show deficits in spatial working memory tasks (Park & Holzman, 1992). These observations suggest that what has been learned from rodent hippocampal studies might be translated into the understanding of human hippocampal functions and might provide inspirations for the study of non-spatial human memories which might share common mechanisms, in turn aiding the development of drugs and therapies for hippocampal-related neurological dysfunctions.

Figure 5.1

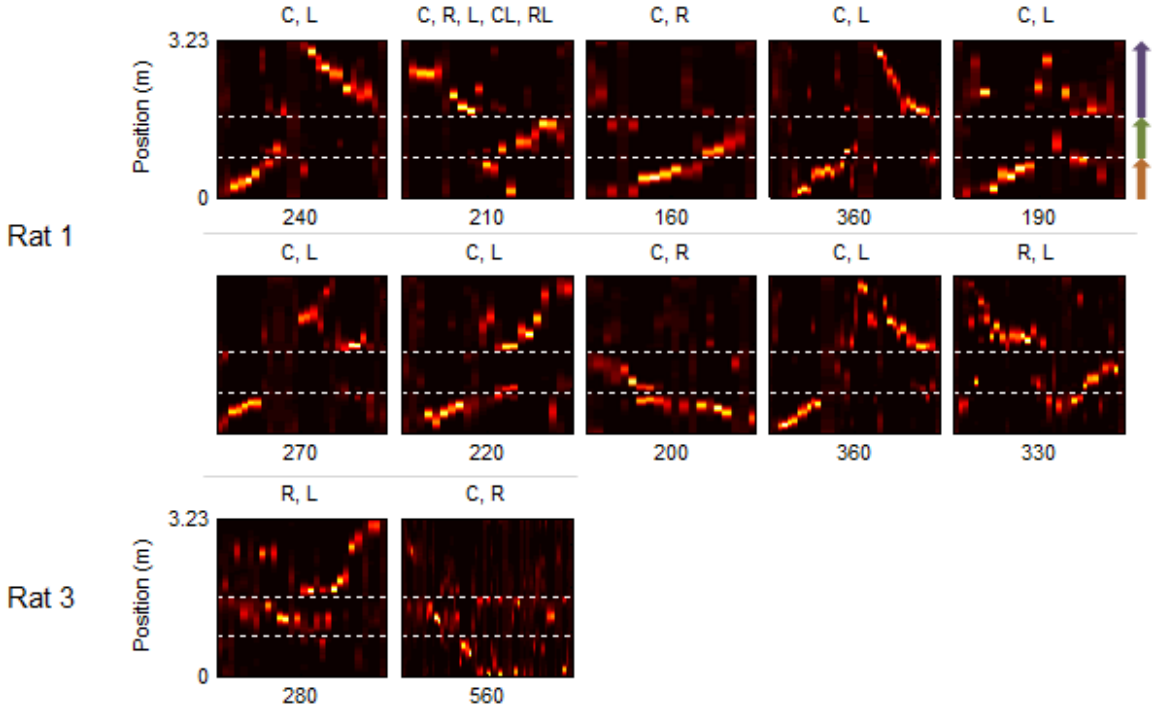

Figure 5.1 Hippocampal replay events did not represent multiple track arms at the same time

Hippocampal population firing (candidate) events determined to represent multiple track arms yet not identified as joint replays are shown (0 events from rat 2). The subregions determined to contain replay structure are noted above each example. Candidate event durations in ms are noted below each example.

Figure 5.2

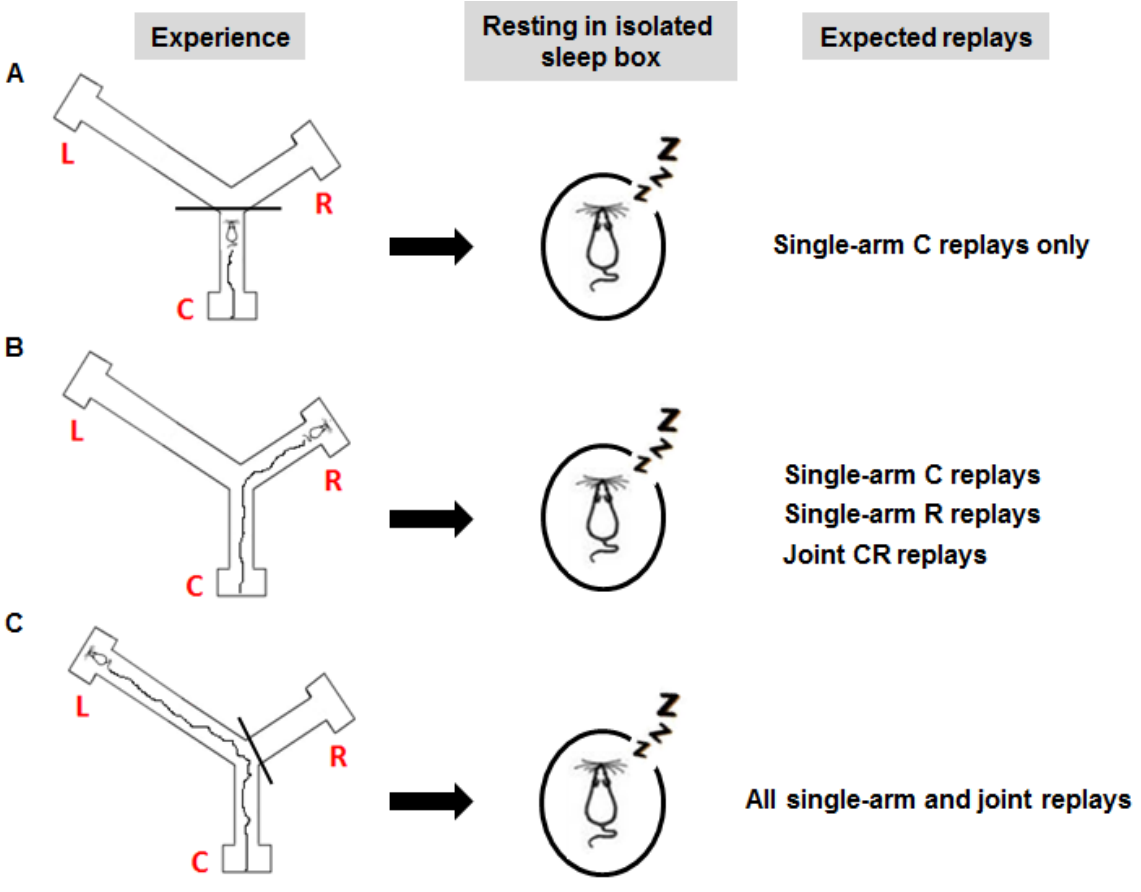

Figure 5.2 A modified experimental design

The first experience of the novel Y maze is divided into three segments of single-lap running, each followed by a resting session in an isolated sleep box with replay representations expected to be observed noted on right. The animal is immediately taken out of the Y maze after a single experience of **(A)** traversal on the C arm, **(B)** the joint CR trajectory, and **(C)** the joint CL trajectory which may be enforced by the experimenter or a barrier blocking off the R arm.

References

Abraham, W.C. (2003) How long will long-term potentiation last? *Philos Trans R Soc Lond B Biol Sci*, **358**, 735-744.

Allport, D.A. (1985) Distributed memory, modular systems and dysphasia. In Newman, S.K., Epstein, R. (eds) *Current Perspectives in Dysphasia*. Churchill Livingstone, Edinburgh.

Andersen, P., Morris, R., Amaral, D., Bliss, T. & O'Keefe, J. (2006) *The Hippocampus Book*. Oxford University Press.

Benchenane, K., Peyrache, A., Khamassi, M., Tierney, P.L., Gioanni, Y., Battaglia, F.P. & Wiener, S.I. (2010) Coherent theta oscillations and reorganization of spike timing in the hippocampal- prefrontal network upon learning. *Neuron*, **66**, 921-936.

Bird, C.M. & Burgess, N. (2008) The hippocampus and memory: insights from spatial processing. *Nat Rev Neurosci*, **9**, 182-194.

Bliss, T.V. & Gardner-Medwin, A.R. (1973) Long-lasting potentiation of synaptic transmission in the dentate area of the unanaestetized rabbit following stimulation of the perforant path. *J Physiol*, **232**, 357-374.

Bliss, T.V. & Lomo, T. (1973) Long-lasting potentiation of synaptic transmission in the dentate area of the anaesthetized rabbit following stimulation of the perforant path. *J Physiol*, **232**, 331-356.

Bostock, E., Muller, R.U. & Kubie, J.L. (1991) Experience-dependent modifications of hippocampal place cell firing. *Hippocampus*, **1**, 193-205.

Brito, G.N., Thomas, G.J., Davis, B.J. & Gingold, S.I. (1982) Prelimbic cortex, mediodorsal thalamus, septum, and delayed alternation in rats. *Exp Brain Res*, **46**, 52-58.

Brown, V.J. & Bowman, E.M. (2002) Rodent models of prefrontal cortical function. *Trends Neurosci*, **25**, 340-343.

Buckner, R.L. (2010) The role of the hippocampus in prediction and imagination. *Annu Rev Psychol*, **61**, 27-48, C21-28.

Buzsaki, G. (1989) Two-stage model of memory trace formation: a role for "noisy" brain states. *Neuroscience*, **31**, 551-570.

Byrne, P., Becker, S. & Burgess, N. (2007) Remembering the past and imagining the future: a neural model of spatial memory and imagery. *Psychol Rev*, **114**, 340-375.

Carr, D.B. & Sesack, S.R. (1996) Hippocampal afferents to the rat prefrontal cortex: synaptic targets and relation to dopamine terminals. *J Comp Neurol*, **369**, 1-15.

Carr, M.F., Jadhav, S.P. & Frank, L.M. (2011) Hippocampal replay in the awake state: a potential substrate for memory consolidation and retrieval. *Nat Neurosci*, **14**, 147-153.

Cohen, N.J., Eichenbaum, H. (1993) *Memory, Amnesia and the Hippocampal System*. MIT Press, Cambridge, Massachusettes.

Corkin, S., Amaral, D.G., Gonzalez, R.G., Johnson, K.A. & Hyman, B.T. (1997) H. M.'s medial temporal lobe lesion: findings from magnetic resonance imaging. *J Neurosci*, **17**, 3964-3979.

Csicsvari, J., Hirase, H., Mamiya, A. & Buzsaki, G. (2000) Ensemble patterns of hippocampal CA3-CA1 neurons during sharp wave-associated population events. *Neuron*, **28**, 585-594.

Csicsvari, J., O'Neill, J., Allen, K. & Senior, T. (2007) Place-selective firing contributes to the reverse-order reactivation of CA1 pyramidal cells during sharp waves in open-field exploration. *Eur J Neurosci*, **26**, 704-716.

Dalley, J.W., Cardinal, R.N. & Robbins, T.W. (2004) Prefrontal executive and cognitive functions in rodents: neural and neurochemical substrates. *Neurosci Biobehav Rev*, **28**, 771-784.

Dan, Y. & Poo, M.M. (1992) Hebbian depression of isolated neuromuscular synapses in vitro. *Science*, **256**, 1570-1573.

Davidson, T.J., Kloosterman, F. & Wilson, M.A. (2009) Hippocampal replay of extended experience. *Neuron*, **63**, 497-507.

De Bruin, J.P., Feenstra, M.G., Broersen, L.M., Van Leeuwen, M., Arens, C., De Vries, S. & Joosten, R.N. (2000) Role of the prefrontal cortex of the rat in learning and decision making: effects of transient inactivation. *Prog Brain Res*, **126**, 103-113.

Deacon, R.M. & Rawlins, J.N. (2006) T-maze alternation in the rodent. *Nat Protoc*, **1**, 7-12.

Diba, K. & Buzsaki, G. (2007) Forward and reverse hippocampal place-cell sequences during ripples. *Nat Neurosci*, **10**, 1241-1242.

Doya, K. (2008) Modulators of decision making. *Nat Neurosci*, **11**, 410-416.

Dragoi, G. & Tonegawa, S. (2011) Preplay of future place cell sequences by hippocampal cellular assemblies. *Nature*, **469**, 397-401.

Dragoi, G. & Tonegawa, S. (2013) Distinct preplay of multiple novel spatial experiences in the rat. *Proc Natl Acad Sci U S A*, **110**, 9100-9105.

Dudai, Y. (2004) The neurobiology of consolidations, or, how stable is the engram? *Annu Rev Psychol*, **55**, 51-86.

Ego-Stengel, V. & Wilson, M.A. (2010) Disruption of ripple-associated hippocampal activity during rest impairs spatial learning in the rat. *Hippocampus*, **20**, 1-10.

Eichenbaum, H. (2013) What H.M. taught us. *J Cogn Neurosci*, **25**, 14-21.

Ekstrom, A.D., Kahana, M.J., Caplan, J.B., Fields, T.A., Isham, E.A., Newman, E.L. & Fried, I. (2003) Cellular networks underlying human spatial navigation. *Nature*, **425**, 184-188.

Fanselow, M.S. & Dong, H.W. (2010) Are the dorsal and ventral hippocampus functionally distinct structures? *Neuron*, **65**, 7-19.

Floresco, S.B., Braaksma, D.N. & Phillips, A.G. (1999) Thalamic-cortical-striatal circuitry subserves working memory during delayed responding on a radial arm maze. *J Neurosci*, **19**, 11061-11071.

Floresco, S.B., Seamans, J.K. & Phillips, A.G. (1997) Selective roles for hippocampal, prefrontal cortical, and ventral striatal circuits in radial-arm maze tasks with or without a delay. *J Neurosci*, **17**, 1880-1890.

Foster, D.J. & Knierim, J.J. (2012) Sequence learning and the role of the hippocampus in rodent navigation. *Curr Opin Neurobiol*, **22**, 294-300.

Foster, D.J. & Wilson, M.A. (2006) Reverse replay of behavioural sequences in hippocampal place cells during the awake state. *Nature*, **440**, 680-683.

Frank, L.M., Brown, E.N. & Wilson, M. (2000) Trajectory encoding in the hippocampus and entorhinal cortex. *Neuron*, **27**, 169-178.

Frank, L.M., Stanley, G.B. & Brown, E.N. (2004) Hippocampal plasticity across multiple days of exposure to novel environments. *J Neurosci*, **24**, 7681-7689.

Gallistel, C.R. (1990) *The organization of learning*. MIT Press, Cambridge, Mass.

Girardeau, G., Benchenane, K., Wiener, S.I., Buzsaki, G. & Zugaro, M.B. (2009) Selective suppression of hippocampal ripples impairs spatial memory. *Nat Neurosci*, **12**, 1222-1223.

Gupta, A.S., van der Meer, M.A., Touretzky, D.S. & Redish, A.D. (2010) Hippocampal replay is not a simple function of experience. *Neuron*, **65**, 695-705.

Hahn, T.T., Sakmann, B. & Mehta, M.R. (2006) Phase-locking of hippocampal interneurons' membrane potential to neocortical up-down states. *Nat Neurosci*, **9**, 1359-1361.

Hebb, D.O. (1949) *The Organization of Behavior*. Wiley & Sons, New York.

Hill, A.J. (1978) First occurrence of hippocampal spatial firing in a new environment. *Exp Neurol*, **62**, 282-297.

Ho, A.S., Hori, E., Nguyen, P.H., Urakawa, S., Kondoh, T., Torii, K., Ono, T. & Nishijo, H. (2011) Hippocampal neuronal responses during signaled licking of gustatory stimuli in different contexts. *Hippocampus*, **21**, 502-519.

Hollup, S.A., Molden, S., Donnett, J.G., Moser, M.B. & Moser, E.I. (2001) Accumulation of hippocampal place fields at the goal location in an annular watermaze task. *J Neurosci*, **21**, 1635-1644.

Hyman, J.M., Zilli, E.A., Paley, A.M. & Hasselmo, M.E. (2005) Medial prefrontal cortex cells show dynamic modulation with the hippocampal theta rhythm dependent on behavior. *Hippocampus*, **15**, 739-749.

Isomura, Y., Sirota, A., Ozen, S., Montgomery, S., Mizuseki, K., Henze, D.A. & Buzsaki, G. (2006) Integration and segregation of activity in entorhinal-hippocampal subregions by neocortical slow oscillations. *Neuron*, **52**, 871-882.

Jacobs, L.F. & Schenk, F. (2003) Unpacking the cognitive map: the parallel map theory of hippocampal function. *Psychol Rev*, **110**, 285-315.

Jay, T.M. & Witter, M.P. (1991) Distribution of hippocampal CA1 and subicular efferents in the prefrontal cortex of the rat studied by means of anterograde transport of Phaseolus vulgaris-leucoagglutinin. *J Comp Neurol*, **313**, 574-586.

Jensen, O. & Lisman, J.E. (1996) Hippocampal CA3 region predicts memory sequences: accounting for the phase precession of place cells. *Learn Mem*, **3**, 279-287.

Ji, D. & Wilson, M.A. (2007) Coordinated memory replay in the visual cortex and hippocampus during sleep. *Nat Neurosci*, **10**, 100-107.

Jones, M.W. (2002) A comparative review of rodent prefrontal cortex and working memory. *Curr Mol Med*, **2**, 639-647.

Jones, M.W. & Wilson, M.A. (2005) Theta rhythms coordinate hippocampal-prefrontal interactions in a spatial memory task. *PLoS Biol*, **3**, e402.

Jung, M.W., Qin, Y., McNaughton, B.L. & Barnes, C.A. (1998) Firing characteristics of deep layer neurons in prefrontal cortex in rats performing spatial working memory tasks. *Cereb Cortex*, **8**, 437-450.

Kable, J.W. & Glimcher, P.W. (2009) The neurobiology of decision: consensus and controversy. *Neuron*, **63**, 733-745.

Karlsson, M.P. & Frank, L.M. (2009) Awake replay of remote experiences in the hippocampus. *Nat Neurosci*, **12**, 913-918.

Kesner, R.P. & Churchwell, J.C. (2011) An analysis of rat prefrontal cortex in mediating executive function. *Neurobiol Learn Mem*, **96**, 417-431.

Koene, R.A. & Hasselmo, M.E. (2008) Reversed and forward buffering of behavioral spike sequences enables retrospective and prospective retrieval in hippocampal regions CA3 and CA1. *Neural Netw*, **21**, 276-288.

Kraus, B.J., Robinson, R.J., 2nd, White, J.A., Eichenbaum, H. & Hasselmo, M.E. (2013) Hippocampal "time cells": time versus path integration. *Neuron*, **78**, 1090-1101.

Kudrimoti, H.S., Barnes, C.A. & McNaughton, B.L. (1999) Reactivation of hippocampal cell assemblies: effects of behavioral state, experience, and EEG dynamics. *J Neurosci*, **19**, 4090-4101.

Lalonde, R. (2002) The neurobiological basis of spontaneous alternation. *Neurosci Biobehav Rev*, **26**, 91-104.

Lansink, C.S., Goltstein, P.M., Lankelma, J.V., McNaughton, B.L. & Pennartz, C.M. (2009) Hippocampus leads ventral striatum in replay of place-reward information. *PLoS Biol*, **7**, e1000173.

Lee, A.K. & Wilson, M.A. (2002) Memory of sequential experience in the hippocampus during slow wave sleep. *Neuron*, **36**, 1183-1194.

Lee, I., Griffin, A.L., Zilli, E.A., Eichenbaum, H. & Hasselmo, M.E. (2006) Gradual translocation of spatial correlates of neuronal firing in the hippocampus toward prospective reward locations. *Neuron*, **51**, 639-650.

Leibold, C. & Kempter, R. (2006) Memory capacity for sequences in a recurrent network with biological constraints. *Neural Comput*, **18**, 904-941.

Lever, C., Wills, T., Cacucci, F., Burgess, N. & O'Keefe, J. (2002) Long-term plasticity in hippocampal place-cell representation of environmental geometry. *Nature*, **416**, 90-94.

Levy, W.B. (1996) A sequence predicting CA3 is a flexible associator that learns and uses context to solve hippocampal-like tasks. *Hippocampus*, **6**, 579-590.

Levy, W.B. & Steward, O. (1983) Temporal contiguity requirements for long-term associative potentiation/depression in the hippocampus. *Neuroscience*, **8**, 791-797.

Louie, K. & Wilson, M.A. (2001) Temporally structured replay of awake hippocampal ensemble activity during rapid eye movement sleep. *Neuron*, **29**, 145-156.

Lynch, G.S., Dunwiddie, T. & Gribkoff, V. (1977) Heterosynaptic depression: a postsynaptic correlate of long-term potentiation. *Nature*, **266**, 737-739.

MacDonald, C.J., Lepage, K.Q., Eden, U.T. & Eichenbaum, H. (2011) Hippocampal "time cells" bridge the gap in memory for discontiguous events. *Neuron*, **71**, 737-749.

Marr, D. (1971) Simple memory: a theory for archicortex. *Philos Trans R Soc Lond B Biol Sci*, **262**, 23-81.

Martin, S.J., Grimwood, P.D. & Morris, R.G. (2000) Synaptic plasticity and memory: an evaluation of the hypothesis. *Annu Rev Neurosci*, **23**, 649-711.

Matsumura, N., Nishijo, H., Tamura, R., Eifuku, S., Endo, S. & Ono, T. (1999) Spatial- and task-dependent neuronal responses during real and virtual translocation in the monkey hippocampal formation. *J Neurosci*, **19**, 2381-2393.

McNaughton, B.L., Battaglia, F.P., Jensen, O., Moser, E.I. & Moser, M.B. (2006) Path integration and the neural basis of the 'cognitive map'. *Nat Rev Neurosci*, **7**, 663-678.

Mehta, M.R., Quirk, M.C. & Wilson, M.A. (2000) Experience-dependent asymmetric shape of hippocampal receptive fields. *Neuron*, **25**, 707-715.

Miller, E.K. & Cohen, J.D. (2001) An integrative theory of prefrontal cortex function. *Annu Rev Neurosci*, **24**, 167-202.

Mishkin, M., Vargha-Khadem, F. & Gadian, D.G. (1998) Amnesia and the organization of the hippocampal system. *Hippocampus*, **8**, 212-216.

Moita, M.A., Rosis, S., Zhou, Y., LeDoux, J.E. & Blair, H.T. (2003) Hippocampal place cells acquire location-specific responses to the conditioned stimulus during auditory fear conditioning. *Neuron*, **37**, 485-497.

Molter, C., Sato, N. & Yamaguchi, Y. (2007) Reactivation of behavioral activity during sharp waves: a computational model for two stage hippocampal dynamics. *Hippocampus*, **17**, 201-209.

Montague, P.R., Dayan, P. & Sejnowski, T.J. (1996) A framework for mesencephalic dopamine systems based on predictive Hebbian learning. *J Neurosci*, **16**, 1936-1947.

Morris, R.G. (2001) Episodic-like memory in animals: psychological criteria, neural mechanisms and the value of episodic-like tasks to investigate animal models of neurodegenerative disease. *Philos Trans R Soc Lond B Biol Sci*, **356**, 1453-1465.

Moser, E.I., Kropff, E. & Moser, M.B. (2008) Place cells, grid cells, and the brain's spatial representation system. *Annu Rev Neurosci*, **31**, 69-89.

Muller, G.E. & Pilzecker, A. (1900) Experimentelle Beitrage zur Lehre von Gedächtnis. *Z. Psychol.*, **1**, 1–300.

Muller, R.U. & Kubie, J.L. (1987) The effects of changes in the environment on the spatial firing of hippocampal complex-spike cells. *J Neurosci*, **7**, 1951-1968.

Nakashiba, T., Buhl, D.L., McHugh, T.J. & Tonegawa, S. (2009) Hippocampal CA3 output is crucial for ripple-associated reactivation and consolidation of memory. *Neuron*, **62**, 781-787.

Nakazawa, K., Sun, L.D., Quirk, M.C., Rondi-Reig, L., Wilson, M.A. & Tonegawa, S. (2003) Hippocampal CA3 NMDA receptors are crucial for memory acquisition of one-time experience. *Neuron*, **38**, 305-315.

O'Keefe, J. (1976) Place units in the hippocampus of the freely moving rat. *Exp Neurol*, **51**, 78-109.

O'Keefe, J. & Dostrovsky, J. (1971) The hippocampus as a spatial map. Preliminary evidence from unit activity in the freely-moving rat. *Brain Res*, **34**, 171-175.

O'Keefe, J. & Nadel, L. (1978) *The Hippocampus As A Cognitive Map*. Clarendon, London.

O'Neill, J., Pleydell-Bouverie, B., Dupret, D. & Csicsvari, J. (2010) Play it again: reactivation of waking experience and memory. *Trends Neurosci*, **33**, 220-229.

O'Neill, J., Senior, T. & Csicsvari, J. (2006) Place-selective firing of CA1 pyramidal cells during sharp wave/ripple network patterns in exploratory behavior. *Neuron*, **49**, 143-155.

O'Neill, J., Senior, T.J., Allen, K., Huxter, J.R. & Csicsvari, J. (2008) Reactivation of experience-dependent cell assembly patterns in the hippocampus. *Nat Neurosci*, **11**, 209-215.

Olton, D.S. & Samuelson, R.J. (1976) Remembrance of places past: spatial memory in rats. *J. Exp. Psychol. Anim. Behav. Process.*, **2**, 97-116.

Owen, G.R. & Brenner, E.A. (2012) Mapping molecular memory: navigating the cellular pathways of learning. *Cell Mol Neurobiol*, **32**, 919-941.

Park, S. & Holzman, P.S. (1992) Schizophrenics show spatial working memory deficits. *Arch Gen Psychiatry*, **49**, 975-982.

Pastalkova, E., Itskov, V., Amarasingham, A. & Buzsaki, G. (2008) Internally generated cell assembly sequences in the rat hippocampus. *Science*, **321**, 1322-1327.

Peyrache, A., Khamassi, M., Benchenane, K., Wiener, S.I. & Battaglia, F.P. (2009) Replay of rule-learning related neural patterns in the prefrontal cortex during sleep. *Nat Neurosci*, **12**, 919-926.

Pfeiffer, B.E. & Foster, D.J. (2013) Hippocampal place-cell sequences depict future paths to remembered goals. *Nature*, **497**, 74-79.

Preuss, T.M. (1995) Do rats have prefrontal cortex? The rose-woolsey-akert program reconsidered. *J Cogn Neurosci*, **7**, 1-24.

Quirk, G.J., Muller, R.U. & Kubie, J.L. (1990) The firing of hippocampal place cells in the dark depends on the rat's recent experience. *J Neurosci*, **10**, 2008-2017.

Quiroga, R.Q., Reddy, L., Kreiman, G., Koch, C. & Fried, I. (2005) Invariant visual representation by single neurons in the human brain. *Nature*, **435**, 1102-1107.

Rasch, B. & Born, J. (2013) About sleep's role in memory. *Physiol Rev*, **93**, 681-766.

Royer, S., Sirota, A., Patel, J. & Buzsaki, G. (2010) Distinct representations and theta dynamics in dorsal and ventral hippocampus. *J Neurosci*, **30**, 1777-1787.

Rugg, M.D., Johnson, J.D., Park, H. & Uncapher, M.R. (2008) Encoding-retrieval overlap in human episodic memory: a functional neuroimaging perspective. *Prog Brain Res*, **169**, 339-352.

Schacter, D.L. & Addis, D.R. (2007) The cognitive neuroscience of constructive memory: remembering the past and imagining the future. *Philos Trans R Soc Lond B Biol Sci*, **362**, 773-786.

Scoville, W.B. & Milner, B. (1957) Loss of recent memory after bilateral hippocampal lesions. *J Neurol Neurosurg Psychiatry*, **20**, 11-21.

Siapas, A.G., Lubenov, E.V. & Wilson, M.A. (2005) Prefrontal phase locking to hippocampal theta oscillations. *Neuron*, **46**, 141-151.

Siapas, A.G. & Wilson, M.A. (1998) Coordinated interactions between hippocampal ripples and cortical spindles during slow-wave sleep. *Neuron*, **21**, 1123-1128.

Singer, A.C. & Frank, L.M. (2009) Rewarded outcomes enhance reactivation of experience in the hippocampus. *Neuron*, **64**, 910-921.

Sirota, A., Csicsvari, J., Buhl, D. & Buzsaki, G. (2003) Communication between neocortex and hippocampus during sleep in rodents. *Proc Natl Acad Sci U S A*, **100**, 2065-2069.

Skaggs, W.E. & McNaughton, B.L. (1996) Replay of neuronal firing sequences in rat hippocampus during sleep following spatial experience. *Science*, **271**, 1870-1873.

Squire, L.R. (1992) Memory and the hippocampus: a synthesis from findings with rats, monkeys, and humans. *Psychol Rev*, **99**, 195-231.

Steinmetz, P.N., Roy, A., Fitzgerald, P.J., Hsiao, S.S., Johnson, K.O. & Niebur, E. (2000) Attention modulates synchronized neuronal firing in primate somatosensory cortex. *Nature*, **404**, 187-190.

Steriade, M., McCormick, D.A. & Sejnowski, T.J. (1993) Thalamocortical oscillations in the sleeping and aroused brain. *Science*, **262**, 679-685.

Swanson, L.W. (1981) A direct projection from Ammon's horn to prefrontal cortex in the rat. *Brain Res*, **217**, 150-154.

Thierry, A.M., Gioanni, Y., Degenetais, E. & Glowinski, J. (2000) Hippocampo-prefrontal cortex pathway: anatomical and electrophysiological characteristics. *Hippocampus*, **10**, 411-419.

Tolman, E.C. (1948) Cognitive maps in rats and men. *Psychol Rev*, **55**, 189-208.

Vertes, R.P. (2006) Interactions among the medial prefrontal cortex, hippocampus and midline thalamus in emotional and cognitive processing in the rat. *Neuroscience*, **142**, 1-20.

Walker, M.P. & Stickgold, R. (2006) Sleep, memory, and plasticity. *Annu Rev Psychol*, **57**, 139-166.

Wang, G.W. & Cai, J.X. (2006) Disconnection of the hippocampal-prefrontal cortical circuits impairs spatial working memory performance in rats. *Behav Brain Res*, **175**, 329-336.

Whitlock, J.R., Heynen, A.J., Shuler, M.G. & Bear, M.F. (2006) Learning induces long-term potentiation in the hippocampus. *Science*, **313**, 1093-1097.

Wilson, M.A. & McNaughton, B.L. (1993) Dynamics of the hippocampal ensemble code for space. *Science*, **261**, 1055-1058.

Wilson, M.A. & McNaughton, B.L. (1994) Reactivation of hippocampal ensemble memories during sleep. *Science*, **265**, 676-679.

Wood, E.R., Dudchenko, P.A. & Eichenbaum, H. (1999) The global record of memory in hippocampal neuronal activity. *Nature*, **397**, 613-616.

Xu, L., Anwyl, R. & Rowan, M.J. (1998) Spatial exploration induces a persistent reversal of long-term potentiation in rat hippocampus. *Nature*, **394**, 891-894.

Yartsev, M.M. & Ulanovsky, N. (2013) Representation of three-dimensional space in the hippocampus of flying bats. *Science*, **340**, 367-372.

Yoo, J.J., Hinds, O., Ofen, N., Thompson, T.W., Whitfield-Gabrieli, S., Triantafyllou, C. & Gabrieli, J.D. (2012) When the brain is prepared to learn: enhancing human learning using real-time fMRI. *Neuroimage*, **59**, 846-852.

Yoon, T., Okada, J., Jung, M.W. & Kim, J.J. (2008) Prefrontal cortex and hippocampus subserve different components of working memory in rats. *Learn Mem*, **15**, 97-105.

CURRICULUM VITAE

Educational History

Ph.D. expected	2014	Program in Neuroscience	Johns Hopkins School of Medicine
B.E.	2007	Biomedical Engineering	Tsinghua University

Other Professional Experience

Conservation Science Network Internship	2013	World Wildlife Fund, Washington D.C.
Research Rotation	2008	Lab of Rüdiger von der Heydt, Johns Hopkins School of Medicine
Research Rotation	2007	Lab of Steve Hsiao, Johns Hopkins School of Medicine
Undergraduate Research Assistant	2006-2007	Lab of Bo Hong, Tsinghua University

Scholarships

Tsinghua University Huang Song-Yi & He Shan-Sheng Outstanding Students' Scholarship, 2006
Tsinghua University Dong Fang Yi De Scholarship for Excellent Academic Performance, 2005
Tsinghua University Chen Zhi-Fu Scholarship for Excellent Academic Performance, 2004
Tsinghua University Third-Level Scholarship for Excellent Performance in Industrial Investigation, 2004

Academic Honors

2005 Second Prize of China Undergraduate Mathematical Contest in Modeling

Peer-reviewed Publications

X. WU, D. J. FOSTER. Hippocampal replay captures the unique topological structure of a novel environment. *In revision, Journal of Neuroscience*

X. WU, D. J. FOSTER. Hippocampal replays modulate prefrontal neuronal activities in a spatial alternation task. *In prep*

L. Feng, **X. Wu**, Z. Qiao, S. Gao, B. Hong. (2007) A real-time auditory neurophysiology toolbox and its application in the study of information encoding in rat inferior colliculus. *Acta Biophysica Sinica* 23(3)

Articles

X. Wu. Current development and existing problems of medical devices industry in Shen Zhen. *China Medical Device Information*, No. 9, 2005

Posters

D. J. FOSTER, **X. WU**. Parsing of extended hippocampal replays in a Y maze. Society for Neuroscience annual conference, 2012

X. WU, D. J. FOSTER. Hippocampal replays modulate prefrontal neuronal activities in a spatial alternation task. Society for Neuroscience annual conference, 2012

X. WU, D. J. FOSTER. Hippocampal replay develops rapidly in an environment with novel spatial structure. Society for Neuroscience annual conference, 2011